OPTIMAL CONTROL OF WAVE-INDUCED VIBRATIONS IN SEMISUBMERSIBLE STRUCTURES WITH FLEXIBLE SUPERSTRUCTURES

by

Debasish Ghosh

Dissertation submitted to the faculty of the
Virginia Polytechnic Institute and State University
in partial fulfillment of the requirements for the degree of

DOCTOR OF PHILOSOPHY

in

Engineering Mechanics

APPROVED:

L. Meirovitch, Chairman

H. J. Kelley

M. F. VanLandingham

A. K. Jakubowski

D. Frederick

April, 1986

Blacksburg, Virginia

OPTIMAL CONTROL OF WAVE-INDUCED VIBRATIONS IN SEMISUBMERSIBLE STRUCTURES WITH FLEXIBLE SUPERSTRUCTURES

by

Debasish Ghosh

Committee Chairman: L. Meirovitch, Engineering Mechanics

(ABSTRACT)

This dissertation is concerned with controlling the motion of a semisubmersible structure induced by high-frequency waves. The structure consists of a rigid platform and a flexible superstructure. Motion of a structure in fluids generates forces depending on the motion itself. The added mass and damping terms stemming from this motion depend on the frequency of motion. It is well known that for a given wave height, the wave energy is distributed according to a Rayleigh distribution. Because mass and damping terms vary with the frequency of the wave motion, there is an infinite number of sets of dynamical equations, one for each frequency in the Rayleigh distribution. Practical considerations make it necessary to discretize the frequency spectrum, so that there are as many dynamical equations as frequency increments. The center frequency in each increment is computed by equipartitioning of the wave energy distribution represented by a Bretschneider spectrum. The excitation forces are estimated for each increment and the design of optimal control is carried out by the Independent Modal-Space Control (IMSC) method. The net control forces can be found by summing the forces associated with each increment. The technique is demonstrated by means of a numerical example in which the wave-induced vibration of a cylindrical platform with a flexible cantilever beam is suppressed.

ACKNOWLEDGEMENTS

I am deeply indebted to Professor Leonard Meirovitch for the many opportunities and guidance he has provided me in the course of my doctoral studies at VPI&SU. His assistance and encouragement is sincerely appreciated.

I am grateful to Drs. D. Frederick, A. K. Jakubowski, H. J. Kelley and H. F. VanLandingham for serving on my examining committee and for their review of this dissertation.

I wish to express my deep appreciation to my parents for their continued encouragement during the course of my education. I also wish to express my appreciation to my beloved wife for her patience and moral support.

Last, but not least I wish to thank Mrs. Susanne Davis for her expert typing of this dissertation.

TABLE OF CONTENTS

LIST OF FIGURES

LIST OF TABLES

CHAPTER I

INTRODUCTION

1.1 PRELIMINARY REMARKS

Civil structures such as suspension bridges, buildings and offshore-structures can undergo large-amplitude vibration in response to environmental forces. The environmental forces can be very large and, if the structure is sufficiently flexible, can lead to discomfort for the occupants and even to failure of the structure. The disaster of the Tacoma Narrows Bridge in the state of Washington, U.S.A., caused by wind-induced forces, is well publicized (Ref. 1). In recent years, successful application of modern control theory to aerospace problems has stirred an interest in the application of active control theory to the vibration suppression in civil structures. Unlike aerospace structures, which are subjected to negligible environmental loads, civil structures are subjected to large environmental loads. For example, buildings are subjected to earthquake and wind loads, whereas offshore structures are subjected to wind and wave loads. In this dissertation, we attempt to control the motion of a semisubmersible structure caused by waves.

In the past, when oil was extracted from fields lying in shallow waters, offshore platforms could be moored to ensure a stable working area. In recent years, there has been a trend toward fields in deeper waters, rendering mooring impractical. This necessitates the positioning of offshore structures by active control, which has given rise to a technique known as "dynamic positioning." However, the effect of envi-

ronmental loads in deeper waters, such as ocean waves, becomes more serious. In the dynamic positioning technique, control forces are generated so as to regulate the motions of a rigid structure caused by low-frequency waves (Ref. 2). The motion generated by high-frequency waves is filtered out and left uncontrolled even though these forces can be very large (Ref. 3). Offshore platforms often support auxiliary structures, such as communication towers and cranes. These auxiliary superstructures are often sufficiently flexible to undergo excessive vibration, and as mentioned earlier can lead to discomfort for the occupants and even to structural failure.

The area of active control of civil structures is still in its early stages and the literature available is scant. As a background for the present work, we present a brief survey of research carried out in related areas.

1.2 LITERATURE SURVEY

In one of the earliest papers in the area of control of civil structures Yang [Ref. 4] applied optimal control theory to the control of building structures subjected to random vibrations arising from earthquake motion and wind loading. This study used equations of motion involving the horizontal motion of the floors only. The performance index was formulated on the basis of structural integrity and economy of energy used in operating the actuators. Although the study was limited to Gaussian white noise, numerical examples showed that significant reduction in variances can be achieved and that structural responses decrease as control forces increase.

Meirovitch and Silverberg (Ref. 5) have studied the control of structures subjected to seismic excitation. They considered complex structures represented by assemblages of distributed components such as beams and columns. Such structures, when modeled by the finite element method, are characterized by a large number of degrees of freedom. Because in practice it is feasible to control only a limited number of modes, a reduced-order controller was developed. The required control law was determined using independent-modal-space-control (IMSC) (Refs. 6,7) and linear optimal control theory (Ref. 8). The investigators presented a simulation study that showed that the structure experienced displacements which were about one-tenth in magnitude compared to an uncontrolled structure. The investigators did not include structural damping, wind loads and the stochastic nature of earthquake excitation.

Meirovitch and Ghosh (Ref. 9) applied optimal control theory to suppress the flutter instability of a suspension bridge by means of feedback control. The partial differential equations of motions, which in the presence of aeroelastic forces are non-self-adjoint, were converted into a set of second-order ordinary differential equations by Galerkin's method. The design of optimal control was carried out by the IMSC method. The closed-loop eigenvalues were selected so that unstable flutter mode acquired a negative real part while the open-loop frequency remained unchanged. The technique was successfully demonstrated by means of numerical example in which the flutter of a suspension bridge deck similar to the Tacoma Narrows Bridge was controlled.

1.3 OUTLINE

This dissertation is concerned with the control of an offshore structure subjected to high-frequency wave forces. To this end, the mathematical model consists of a floating rigid platform and a flexible superstructure attached to the platform. Motion of a structure in fluids generates forces depending on the motion itself. This gives rise to added mass and damping terms depending on the frequency of motion. Also, the damping terms render the system non-self-adjoint. If the flexible superstructure is much lighter than the platform, the motion of the rigid platform affects the vibration of the flexible structure, but not vice-versa. The motion of the rigid platform is described by ordinary differential equations and the vibration of the superstructure relative to the platform can be described by partial differential equations. Practical considerations dictate that the system be approximated by one consisting entirely of ordinary differential equations. To this end, the flexible superstructure is discretized by the finite element method and the equations of motion are derived by the Lagrangian approach. The system can be controlled by the Independent Modal-Space Control (IMSC) method (Refs. 5-7).

It is well known that for a given wave height, the wave energy is distributed according to a Rayleigh distribution (Ref. 2). Because the mass and damping terms vary with the frequency of the wave motion, there is an infinite number of sets of dynamical equations, one for each frequency in the Rayleigh distribution range. In view of the fact that it is not possible to work with an infinite number of sets of dynamical equations, it is necessary to discretize the frequency spectrum, so that

there are as many sets of dynamical equations as frequency increments. The mass and damping can be assumed to remain constant over each increment and can be represented by the values of mass and damping corresponding to the center frequency of each increment. The center frequencies are computed by equipartitioning of the wave energy distribution represented by a Bretschneider spectrum (Ref. 2). The excitation forces are estimated for each increment and the design of optimal control is carried out by the IMSC method. Because the excitation forces can only be estimated, it is necessary to design an observer for each interval to take into account the deviations from actual excitation forces. The net control forces can be found by summing the forces associated with each increment. The technique is demonstrated for a typical increment by a numerical example.

CHAPTER II

DERIVATION OF THE EQUATIONS OF MOTION

2.1 INTRODUCTION

In this chapter, Lagrange's equations of motion for the entire structure are derived by assuming that the semisubmersible consists of a rigid platform and a flexible superstructure. The motion of the rigid platform is described by ordinary differential equations and the vibration of the flexible superstructure relative to the platform can be described by linear partial differential equations. Hence, assuming small rigid-body motions, the complete equations of motion describing a semisubmersible structure is a set of hybrid linear differential equations.

In general hybrid systems of equations do not admit closed-form solutions. Approximate solutions can be obtained via spatial discretization, which yields a set of ordinary differential equations. In one class of spatial discretization method, coordinates describing the motion of the flexible structure are assumed in the form of series of space-dependent admissible functions multiplied by time-dependent generalized coordinates. An exact description of the system dynamics requires an infinite number of terms in the series for the elastic displacements, thus yielding infinite-dimensional coefficient matrices for the discretized model. For practical reasons, it is necessary to retain a finite number of terms in the series representation. Of course, the truncation must be performed such that the basic dynamic characteristics of the system are not sacrificed. The foregoing

procedure of spatial discretization and truncation is called the classical Rayleigh-Ritz method. The drawback of this method is that it requires admissible functions defined over the entire domain of the flexible structure, i.e., global admissible functions. For systems with complex geometry, it is difficult to produce satisfactory global admissible functions valid for the entire domain. In another method of spatial discretization known as the finite element method, the admissible functions are defined over small subdomains instead of the entire domain i.e., they are local admissible functions. The finite element method permits the application of the method to systems with complex geometries. Moreover, it permits the use of very simple admissible functions. In this dissertation, we choose the finite element method for discretizing the flexible structure.

2.2 KINEMATICAL CONSIDERATIONS

We wish to derive the equations of motion for a rigid semisubmerged platform with a flexible superstructure, as shown in Fig. 2.1. To this end, we consider an inertial frame, XYZ with the origin at O' and introduce a reference frame xyz with the origin at the center of mass O of the entire structure in undeformed state; the frame xyz is rigidly attached to the platform. The position of a point in the rigid platform is represented by the vector $\underset{\sim}{r}$ with respect to O. The position of a point in the undeformed flexible superstructure is represented by the vector $\underset{\sim}{r}$ given by

$$\underset{\sim}{r} = \underset{\sim}{R}_O + \underset{\sim}{r}_E + \underset{\sim}{\rho} \tag{2.1}$$

where, $\underset{\sim}{R}_O$ is the vector from O' to O, $\underset{\sim}{r}_E$ is the position vector of a

point E on the boundary between the rigid structure and flexible superstructure and $\underset{\sim}{\rho}$ is the position vector of a typical point in the flexible structure with respect to E. Denoting by $\underset{\sim}{u}$ the elastic displacement of a point in the flexible superstructure, the position of a point in the deformed structure is

$$\underset{\sim}{r} = \underset{\sim}{R}_0 + \underset{\sim}{r}_E + \underset{\sim}{\rho} + \underset{\sim}{u} \tag{2.2}$$

The velocity $\underset{\sim}{v}$ of a point $\underset{\sim}{r}$ in the rigid body in terms of components along the body frame is

$$\underset{\sim}{u} = \dot{\underset{\sim}{R}}_0 + \dot{\underset{\sim}{v}} = \underset{\sim}{V}_0 + \underset{\sim}{\omega}\times\underset{\sim}{r} \tag{2.3}$$

Where $\underset{\sim}{V}_0$ is the velocity of origin O of the body frame and $\underset{\sim}{\omega}$ is the angular velocity of xyz in terms of components along the body frame.

The velocity of a point in the flexible structure is given by

$$\underset{\sim}{v} = \dot{\underset{\sim}{R}}_0 + \underset{\sim}{\omega}\times(\underset{\sim}{r}_E + \underset{\sim}{\rho} + \underset{\sim}{u}) + \dot{\underset{\sim}{u}} \tag{2.4}$$

where $\dot{\underset{\sim}{u}}$ is the elastic velocity of the point relative to the body frame. For small values of $\underset{\sim}{\omega}$ and $\underset{\sim}{u}$, the product $\underset{\sim}{\omega}\times\underset{\sim}{u}$ is of second order in magnitude and can be ignored, so that

$$\underset{\sim}{v} = \dot{\underset{\sim}{R}}_0 + \underset{\sim}{\omega}\times(\underset{\sim}{r}_E + \underset{\sim}{\rho}) + \dot{\underset{\sim}{u}} \tag{2.5}$$

2.3 KINETIC AND POTENTIAL ENERGY

We propose to derive the Lagrange's equations of motion by means of the extended Hamilton's principle. This requires expressions for the kinetic energy, potential energy and virtual work.

The equations of motion consist of six ordinary differential equations for the rigid-body motions and a set of partial differential equations for the elastic members of the superstructure. Instead of working with a hybrid set of equations, we propose to discretize the

structure in space, before the equations are actually derived. To this end, we use the finite element method.

The kinetic energy, T_R of the rigid structure has the expression

$$T_R = \frac{1}{2}\int_{m_R} (\underset{\sim}{V}_0 + \underset{\sim}{\omega} \times \underset{\sim}{r}_R)\cdot(\underset{\sim}{V}_0 + \underset{\sim}{\omega} \times \underset{\sim}{r}_R)dm_R$$

$$= \frac{1}{2}\int_{m_R} [\underset{\sim}{V}_0\cdot\underset{\sim}{V}_0 + 2\underset{\sim}{V}_0\cdot(\underset{\sim}{\omega} \times \underset{\sim}{r}_R) + (\underset{\sim}{\omega} \times \underset{\sim}{r}_R)\cdot(\underset{\sim}{\omega} \times \underset{\sim}{r}_R)]dm_R \qquad (2.6)$$

where m_R is the mass of the rigid structure. Moreover, considering n finite elements, the kinetic energy T_F of the flexible structure can be written as

$$T_F = \frac{1}{2}\sum_{i=1}^{n}\int_{m_i}\{\underset{\sim}{V}_0\cdot\underset{\sim}{V}_0 + 2\underset{\sim}{V}_0\cdot[\underset{\sim}{\omega}\times(\underset{\sim}{r}_E + \underset{\sim}{\rho}_i)] + 2\underset{\sim}{V}_0\cdot\dot{\underset{\sim}{u}}_i$$
$$+ [\underset{\sim}{\omega}\times(\underset{\sim}{r}_E + \underset{\sim}{\rho}_i)]\cdot[\underset{\sim}{\omega}\times(\underset{\sim}{r}_E + \underset{\sim}{\rho}_i)] + 2[\underset{\sim}{\omega}\times(\underset{\sim}{r}_E + \underset{\sim}{\rho}_i)]\cdot\dot{\underset{\sim}{u}}_i$$
$$+ (\dot{\underset{\sim}{u}}_i\cdot\dot{\underset{\sim}{u}}_i)\}dm_i \qquad (2.7)$$

where m_i is the mass of the ith element. The total kinetic energy is obtained by combining Eqs. (2.6) and (2.7), so that

$$T = T_R + T_F = \frac{1}{2m}\underset{\sim}{V}_0\cdot\underset{\sim}{V}_0 + \underset{\sim}{V}_0\cdot\underset{\sim}{\omega}\times[\int_{m_R}\underset{\sim}{r}\,dm_R + \sum_{i=1}^{n}\int_{m_i}(\underset{\sim}{r}_E + \underset{\sim}{\rho}_i)dm_i]$$
$$+ \frac{1}{2}\int_{m_R}(\underset{\sim}{\omega}\times\underset{\sim}{r})\cdot(\underset{\sim}{\omega}\times\underset{\sim}{r})dm_R + \underset{\sim}{V}_0\cdot\sum_{i=1}^{n}\int_{m_i}\dot{\underset{\sim}{u}}_i\,dm_i$$
$$+ \frac{1}{2}\sum_{i=1}^{n}\int_{m_i}[\underset{\sim}{\omega}\times(\underset{\sim}{r}_E + \underset{\sim}{\rho}_i)]\cdot[\underset{\sim}{\omega}\times(\underset{\sim}{r}_E + \underset{\sim}{\rho}_i)]dm_i$$
$$+ \sum_{i=1}^{n}\int_{m_i}[\underset{\sim}{\omega}\times(\underset{\sim}{r}_E + \underset{\sim}{\rho}_i)]\cdot\dot{\underset{\sim}{u}}_i\,dm_i + \sum_{i=1}^{n}\int_{m_i}\dot{\underset{\sim}{u}}_i\cdot\dot{\underset{\sim}{u}}_i\,dm_i \qquad (2.8)$$

where m is the total mass of the structure. Our object is to express the kinetic energy in terms of nodal velocities. To this end, we assume

that

$$\underset{\sim}{u}_i = L_i \underset{\sim}{q}_i^* = L_i R_i \underset{\sim}{q}_i \tag{2.9}$$

where L_i is a matrix of interpolation functions, R_i is a matrix of direction cosines and $\underset{\sim}{q}_i^*$ and $\underset{\sim}{q}_i$ are nodal displacement vectors for the ith element in terms of local coordinates and global coordinates, respectively. Substitution of Eq. (2.9) into (2.8) yields

$$T = \frac{1}{2} m \underset{\sim}{V}_0^T \underset{\sim}{V}_0 - \underset{\sim}{V}_0^T \tilde{\omega} \underset{\sim}{B} + \sum_{i=1}^{n} \underset{\sim}{V}_0^T \phi_i \dot{\underset{\sim}{q}}_i + \frac{1}{2} \underset{\sim}{\omega}^T I_0 \underset{\sim}{\omega}$$

$$- \sum_{i=1}^{n} \int \dot{\underset{\sim}{q}}_i^T R_i L_i^T \tilde{\omega} (\underset{\sim}{r}_E + \underset{\sim}{\rho}_i) dm_i + \frac{1}{2} \sum_{i=1}^{n} \dot{\underset{\sim}{q}}_i^T \bar{\phi}_i \dot{\underset{\sim}{q}}_i \tag{2.10}$$

where I_0 is the moment of inertia of the entire body about 0 and

$$\underset{\sim}{B} = \int_{m_R} \underset{\sim}{r} \, dm_R + \sum_{i=1}^{n} \int_{m_i} (\underset{\sim}{r}_E + \underset{\sim}{\rho}_i) dm_i \tag{2.11a}$$

$$\phi_i = \int_{m_i} L_i R_i \, dm_i, \quad \bar{\phi}_i = \int_{m_i} R_i L_i^T L_i R_i \, dm_i \tag{2.11b,c}$$

and

$$\tilde{\omega} = \begin{bmatrix} 0 & \omega_z & -\omega_y \\ -\omega_z & 0 & \omega_x \\ \omega_y & -\omega_x & 0 \end{bmatrix} \tag{2.11d}$$

in which ω_x, ω_y, ω_z are the components of $\underset{\sim}{\omega}$.

Then, introducing the notation

$$\tilde{B} = \begin{bmatrix} 0 & B_z & -B_y \\ -B_z & 0 & B_x \\ B_y & -B_x & 0 \end{bmatrix} = - \tilde{B}^T \tag{2.12a}$$

and

$$\tilde{\Phi}_i^T = \int_{m_i} R_i L_i^T (\tilde{r}_E + \tilde{\rho}_i) dm_i \tag{2.12b}$$

in which $\tilde{r}_E$ and $\tilde{\rho}_i$ are skew symmetric matrices of the type (2.12a), the kinetic energy can be written as

$$T = \frac{1}{2} m \underset{\sim}{V}_0^T \underset{\sim}{V}_0 + \underset{\sim}{V}_0^T \tilde{B} \underset{\sim}{\omega} + \dot{\underset{\sim}{q}}^T \Phi^T \underset{\sim}{V}_0 + \frac{1}{2} \underset{\sim}{\omega}^T I_0 \underset{\sim}{\omega} + \dot{\underset{\sim}{q}}^T \tilde{\Phi}^T \underset{\sim}{\omega} + \frac{1}{2} \dot{\underset{\sim}{q}}^T \bar{\Phi} \dot{\underset{\sim}{q}} \tag{2.13}$$

where Φ, $\tilde{\Phi}$ and $\bar{\Phi}$ are obtained by assembling ϕ_i, $\tilde{\phi}_i$ and $\bar{\phi}_i$ respectively.

Next, we derive an expression for the potential energy V in terms of nodal displacements $\underset{\sim}{q}$ of the flexible structure and the generalized rigid-body displacements $\underset{\sim}{S}$ of the rigid structure expressed as

$$\underset{\sim}{S} = \begin{bmatrix} \underset{\sim}{R}_0 \\ \hline \underset{\sim}{\theta} \end{bmatrix} \tag{2.14}$$

To this end V can be written symbolically as

$$V = \frac{1}{2}[\underset{\sim}{u},\underset{\sim}{u}] + \frac{1}{2}[\underset{\sim}{S},\underset{\sim}{S}] \tag{2.15}$$

where $[\underset{\sim}{u},\underset{\sim}{u}]$ and $[\underset{\sim}{S},\underset{\sim}{S}]$ are energy inner products (Ref. 9). Using Eq. (9), the potential energy can be written as

$$V = \frac{1}{2} \sum_{i=1}^{n} \underset{\sim}{q}_i^T K_i \underset{\sim}{q}_i + \frac{1}{2} \underset{\sim}{S}^T K_R \underset{\sim}{S} \tag{2.16}$$

where

$$K_i = [L_i R_i, L_i R_i], \quad i = 1,2,\ldots n \tag{2.17a}$$

and

$$K_R = \begin{bmatrix} K_{R1} & K_{R2} \\ \hline K_{R3} & K_{R4} \end{bmatrix} \tag{2.17b}$$

in which K_R is the stiffness matrix of hydrodynamic spring constants, K_{R1} and K_{R4} are matrices of hydrodynamic stiffness coefficients for

linear and angular displacements, respectively, and $K_{R2} = K_{R3}$ is the matrix of coupled stiffness coefficients. Equation (2.16) can be rewritten as

$$V = \frac{1}{2} \underset{\sim}{q}^T K_F \underset{\sim}{q} + \frac{1}{2} \underset{\sim}{S}^T K_R \underset{\sim}{S} \tag{2.18}$$

where K_F is obtained by assembling the element matrices K_i.

Finally, we write expressions for the virtual work due to external forces, including control forces. Denoting the force and moment vectors per unit volume of the rigid structure by $\underset{\sim}{f}_R$ and $\underset{\sim}{f}_{\theta R}$, respectively, and the force and moment vectors per unit volume of the ith element of the flexible structure by $\underset{\sim}{f}_{ui}$ and $\underset{\sim}{f}_{\theta i}(i = 1,2,\ldots n)$, respectively, we can write the virtual work as follows:

$$\delta W = \int_{D_R} [\underset{\sim}{f}_R \cdot \delta(\underset{\sim}{R}_0 + \underset{\sim}{r}) + \underset{\sim}{f}_{\theta R} \cdot \delta\underset{\sim}{\theta}] dD_R + \sum_{i=1}^{n} \int_{D_i} [\underset{\sim}{f}_{ui} \cdot \delta(\underset{\sim}{R}_0 + \underset{\sim}{r}_i) + \underset{\sim}{f}_{\theta i} \cdot \delta(\underset{\sim}{\theta} + \underset{\sim}{\theta}_{fi})] dD_i \tag{2.19}$$

where $\underset{\sim}{\theta}_{fi}$ is the rotation of the cross-section at

$$\underset{\sim}{r}_i = \underset{\sim}{r}_E + \underset{\sim}{\rho}_i + \underset{\sim}{u}_i \tag{2.20}$$

Moreover, D_i is the domain of extension of the ith element of the flexible superstructure. Equation (2.19) can be written as

$$\delta W = \underset{\sim}{F}_0^T \delta\underset{\sim}{R}_0 + \underset{\sim}{M}_0^T \delta\underset{\sim}{\theta} + \sum_{i=1}^{n} \underset{\sim}{Q}_i^T \delta\underset{\sim}{q}_i \tag{2.21}$$

where

$$\underset{\sim}{F}_0 = \int_{D_R} \underset{\sim}{f}_R \, dD_R + \sum_{i=1}^{n} \int_{D_i} \underset{\sim}{f}_{ui} \, dD_i \tag{2.22a}$$

$$\underset{\sim}{M}_0 = \int_{D_R} (\tilde{r}^T \underset{\sim}{f}_R + \underset{\sim}{f}_{\theta R}) dD_R + \sum_{i=1}^{n} \int_{D_i} [(\tilde{r}_E^T + \tilde{\rho}_i^T) \underset{\sim}{f}_{ui} + \underset{\sim}{f}_{\theta i}] dD_i \tag{2.22b}$$

$$\underset{\sim}{Q}_i = \int_{D_i} R_i L_i^T \underset{\sim}{f}_i \, dD_i \tag{2.22c}$$

in which $\underset{\sim}{f}_{ui} = [\underset{\sim}{f}_{ui}^T \quad \underset{\sim}{f}_{\theta i}^T]^T$ (2.22d)

are the generalized force vectors in which $\underset{\sim}{f}_{ui}$ and $\underset{\sim}{f}_{\theta i}$ are the force and moment vectors per unit volume, respectively, for the ith element of the superstructure. Equation (2.21) can be written in the compact form

$$\delta W = \underset{\sim}{F}^T \delta \underset{\sim}{S} + \underset{\sim}{Q}^T \delta \underset{\sim}{q} \tag{2.23}$$

where

$$\underset{\sim}{F} = \begin{bmatrix} \underset{\sim}{F}_O \\ \underset{\sim}{M}_O \end{bmatrix} \tag{2.24}$$

Moreover, $\underset{\sim}{q}$ is the nodal displacement vector and $\underset{\sim}{Q}$ is the vector of nodal forces for the flexible structure and is obtained by assembling $\underset{\sim}{Q}_i$. The vector $\underset{\sim}{F}$ in Eq. (2.23) includes contributions due to the reaction force $\underset{\sim}{F}_r$ arising from the motion of the rigid structure in water, the environmental excitation force $\underset{\sim}{F}_e$ and the control force $\underset{\sim}{F}_c$, so that

$$\underset{\sim}{F} = \underset{\sim}{F}_r + \underset{\sim}{F}_e + \underset{\sim}{F}_c \tag{2.25}$$

where $\underset{\sim}{F}_e$ includes contributions from various sources and can be written as

$$\underset{\sim}{F}_e = \underset{\sim}{F}_f + \underset{\sim}{F}_{ad} + \underset{\sim}{F}_d \tag{2.26}$$

in which $\underset{\sim}{F}_f$ is the generalized hydrodynamic force vector due to disturbances generated in the farfield, $\underset{\sim}{F}_{ad}$ is the generalized aerodynamic force vector and

$$\underset{\sim}{F}_d = \begin{bmatrix} \sum_{i=1}^{n} \underset{\sim}{f}_{ui} dD_i \\ \hline \sum_{i=1}^{n} \int (\tilde{r}_E^T + \tilde{\rho}_i^T) \underset{\sim}{f}_{ui} dD_i + \sum_{i=1}^{n} \underset{\sim}{f}_{\theta i} dD_i \end{bmatrix} \tag{2.27}$$

is the generalized force vector due to distributed forces $\underset{\sim}{f}_{ui}$ and $\underset{\sim}{f}_{\theta i}$ acting on the flexible structure. Also, the control force $\underset{\sim}{F}_c$ in Eq. (2.25) can be expressed as

$$\underset{\sim}{F}_c = \underset{\sim}{F}_{cR} + \underset{\sim}{F}_{cF} \tag{2.28}$$

where $\underset{\sim}{F}_{cR}$ is the generalized control force vector on the rigid body and

$$\underset{\sim}{F}_{cF} = \begin{bmatrix} \sum_{i=1}^{n} \underset{\sim}{f}_{c_{ui}} \\ \hline \sum_{i=1}^{n} \tilde{r}_i^T \underset{\sim}{f}_{c_{ui}} + \sum_{i=1}^{n} \underset{\sim}{f}_{c_{\theta i}} \end{bmatrix} \tag{2.29}$$

is the generalized control force vector due to control forces $\underset{\sim}{f}_{c_{ui}}$ and $\underset{\sim}{f}_{c_{\theta i}}$ acting at the nodes of the flexible structure. Finally, $\underset{\sim}{Q}$ in Eq. (2.23) can be written as

$$\underset{\sim}{Q} = \underset{\sim}{Q}_e + \underset{\sim}{Q}_c \tag{2.30}$$

where $\underset{\sim}{Q}_e$ is the generalized environmental force vector acting on the flexible structure and $\underset{\sim}{Q}_c$ is the generalized control force vector with components acting at the nodes of the flexible structure.

2.4 EQUATIONS OF MOTION

The expressions developed for the kinetic energy, potential energy and virtual work can be used to derive Lagrange's equations of motion, which can be written in the symbolic form

$$\frac{d}{dt}\left(\frac{\partial T}{\partial \underset{\sim}{V}_0}\right) + \frac{\partial V}{\partial \underset{\sim}{R}_0} = \underset{\sim}{F}_0 \tag{2.31a}$$

$$\frac{d}{dt}\left(\frac{\partial T}{\partial \underset{\sim}{\omega}}\right) + \frac{\partial V}{\partial \underset{\sim}{\theta}} = \underset{\sim}{M}_0 \tag{2.31b}$$

$$\frac{d}{dt}\left(\frac{\partial T}{\partial \dot{\underset{\sim}{q}}}\right) + \frac{\partial V}{\partial \underset{\sim}{q}} = \underset{\sim}{Q} \tag{2.31c}$$

Substitution of Eqs. (2.13) and (2.18) into Eqs. (2.31) yields

$$m\dot{\underset{\sim}{V}}_0 + \tilde{\underset{\sim}{B}}\dot{\underset{\sim}{\omega}} + \Phi\ddot{\underset{\sim}{q}} + K_{R1}^T \underset{\sim}{R}_0 + K_{R2}^T \underset{\sim}{\theta} = \underset{\sim}{F}_0 \tag{2.32a}$$

$$\tilde{\underset{\sim}{B}}\dot{\underset{\sim}{V}}_0 - I_0\dot{\underset{\sim}{\omega}} + \tilde{\Phi}\ddot{\underset{\sim}{q}} - K_{R2}^T \underset{\sim}{R}_0 - K_{R4}^T \underset{\sim}{\theta} = -\underset{\sim}{M}_0 \tag{2.32b}$$

$$\Phi^T \dot{V}_0 + \tilde{\Phi}^T \dot{\omega} + \bar{\Phi} \ddot{q} + K_F^T q = Q \tag{2.32c}$$

where K_F is an $\ell \times \ell$ matrix obtained by assembling K_i. Equations (2.32) can be written in a more compact form,

$$M^* \ddot{u}^* + K^* u^* = F^* \tag{2.33}$$

where

$$u^* = [S^T \; q^T]^T \tag{2.34a}$$

$$M^* = \begin{bmatrix} M & \tilde{B} & \Phi \\ -\tilde{B} & I_0 & -\tilde{\Phi}^T \\ \Phi^T & \tilde{\Phi}^T & \bar{\Phi} \end{bmatrix} \tag{2.34b}$$

is a $(6 + \ell) \times (6 + \ell)$ positive definite matrix,

$$K^* = \begin{bmatrix} K_R & 0 \\ 0 & K_F \end{bmatrix} \tag{2.34c}$$

is a positive semidefinite matrix and

$$F^* = \begin{bmatrix} F_0 \\ M_0 \\ Q \end{bmatrix} = \begin{bmatrix} F \\ Q \end{bmatrix} \tag{2.34d}$$

As mentioned earlier, the generalized force vector F includes a component F_r arising from the motion of the structure in water. In general, it depends on the generalized velocity $\dot{S}$ and acceleration $\ddot{S}$ of the rigid structure (Ref. 11) and can be written symbolically as

$$F_r = F_r(S, \dot{S}, \ddot{S}) \tag{2.35}$$

The linearized form of Eq. (2.35) can be written as

$$\underset{\sim}{F}_r = -M_a \ddot{\underset{\sim}{S}} - C_a \dot{\underset{\sim}{S}} \tag{2.36}$$

where M_a is the added mass matrix and C_a is the added damping matrix. In general both matrices depend on the frequency of oscillation of the structure (see Fig. 2.2). Introducing Eq. (2.36) into (2.33) and using Eqs. (2.25) and (2.30), we obtain

$$[M^* + M_a^*]\ddot{\underset{\sim}{u}}^* + C^*\dot{\underset{\sim}{u}}^* + K^*\underset{\sim}{u}^* = \underset{\sim}{F}_e^* + \underset{\sim}{F}_c^* \tag{2.37}$$

where

$$M_a^* = \left[\begin{array}{c|c} M_a & 0 \\ \hline 0 & 0 \end{array}\right] \tag{2.38a}$$

$$C^* = \left[\begin{array}{c|c} C_a & 0 \\ \hline 0 & 0 \end{array}\right] \tag{2.38b}$$

$$K^* = \left[\begin{array}{c|c} K_R & 0 \\ \hline 0 & 0 \end{array}\right] \tag{2.38c}$$

$$\underset{\sim}{F}_e^* = \left[\begin{array}{c} \underset{\sim}{F}_e \\ \hline \underset{\sim}{Q}_e \end{array}\right] \tag{2.38d}$$

$$\underset{\sim}{F}_c^* = \left[\begin{array}{c} \underset{\sim}{F}_c \\ \hline \underset{\sim}{Q}_c \end{array}\right] \tag{2.38e}$$

In general, $\underset{\sim}{F}_e^*$ depends on significant wave height, the angle of incidence of the wave, speed and direction of the current, and speed and direction of the wind. Significant wave height is defined as the average of the one-third highest waves (Ref. 2).

For control purposes, it is convenient to express the equations of motion in state space form. To this end, Eq. (2.37) can be written as

$$M\dot{\underset{\sim}{x}}^* + K\underset{\sim}{x}^* = \underset{\sim}{X}_e^* + \underset{\sim}{X}_c^* \tag{2.39}$$

where

$$M = \left[\begin{array}{c|c} M^* + M_a^* & 0 \\ \hline 0 & I_0 \end{array}\right] \tag{2.40a}$$

$$K = \left[\begin{array}{c|c} C^* & K^* \\ \hline -I & 0 \end{array}\right] \tag{2.40b}$$

$$\underset{\sim}{x}^* = \left[\begin{array}{c} \dot{\underset{\sim}{u}}^* \\ \hline \underset{\sim}{u}^* \end{array}\right] \tag{2.40c}$$

$$\underset{\sim e}{X}^* = \left[\begin{array}{c} \underset{\sim e}{F}^* \\ \hline \underset{\sim}{0} \end{array}\right] \tag{2.40d}$$

$$\underset{\sim c}{X}^* = \left[\begin{array}{c} \underset{\sim c}{F}^* \\ \hline \underset{\sim}{0} \end{array}\right] \tag{2.40e}$$

If M_a is symmetric, then M can be decomposed by the Cholesky decomposition (Ref. 10), i.e., we can write M in the form

$$M = LL^T \tag{2.41}$$

where L is a lower triangular matrix

Introducing Eq. (2.41) into (2.39) and premultiplying by L^{-1} yields

$$L^T \dot{\underset{\sim}{x}}^* + L^{-1} K \underset{\sim}{x}^* = L^{-1} \underset{\sim e}{X}^* + L^{-1} \underset{\sim c}{X}^* \tag{2.42}$$

Then, using the transformation

$$\underset{\sim}{x} = L^T \underset{\sim}{x}^* \tag{2.43}$$

Eq. (2.42) can be written as

$$\dot{\underset{\sim}{x}}(t) = A \underset{\sim}{x}(t) + \underset{\sim e}{P} + \underset{\sim c}{P} \tag{2.44}$$

where

$$A = -L^{-1} K L^{-T} , \tag{2.45a}$$

$$\underset{\sim}{P}_e = L^{-1}\underset{\sim}{X}^*_e \ , \tag{2.45b}$$

$$\underset{\sim}{P}_c = L^{-1}\underset{\sim}{X}^*_c \tag{2.45c}$$

2.4 CONCLUDING REMARKS

Equation (2.44) represents the equations of motion of the system in state-space form. In Chapter 3 the wave spectrum is discretized into a finite number of segments so that there is a state-equation for each segment. The state-equations derived for each segment is then used for the design of controllers and observers. This is done in Chapter 4.

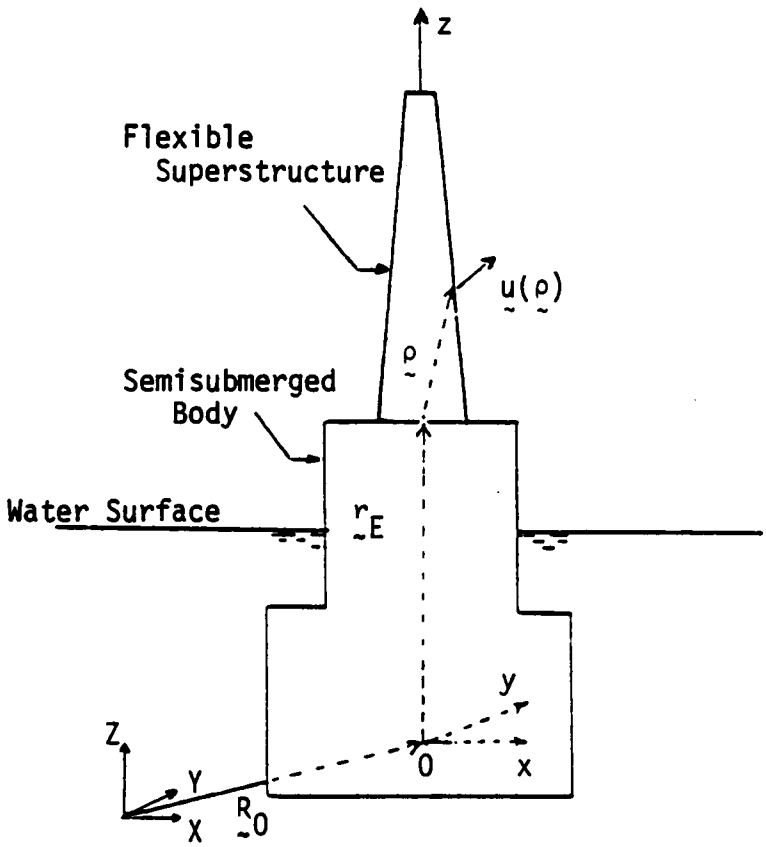

Fig. 2.1 - A Semisubmersible Structure

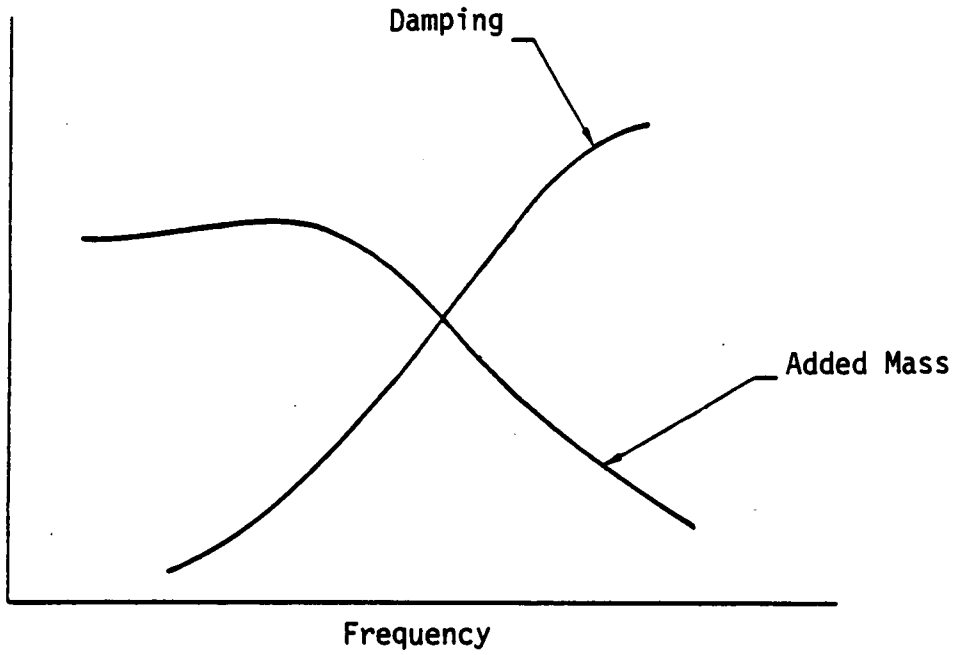

Fig. 2.2 - Hydrodynamic Parameters vs Frequency

CHAPTER III

ESTIMATION OF THE WAVE FORCES

3.1 INTRODUCTION

An offshore vessel at sea is subjected to disturbance forces which cause the vessel to move and change its heading. The most common environmental disturbance acting on a vessel are the wind, the waves and the sea currents. In this paper, we restrict ourselves to the control of motion generated by wind-induced waves. The analysis can be extended so as to include the other effects.

As wind moves over the surface of the sea, it interacts with the water surface to form waves. The strength of the waves depends on the wind speed and duration and on the area over which the wind blows. An increase in any one of these factors results in stronger waves, i.e., waves with larger mean wave height. They can be described mathematically by a random spectrum, which is essentially a Rayleigh distribution (Fig. 3.1). There are various models available for describing the wave spectrum. A spectrum that is widely used is the Bretschneider spectrum (Ref. 2) which is described in Section 3.2.

As remarked earlier, added mass and damping terms, stemming from the motion of the structure in water, depend on the frequency of oscillation. This necessitates the discretization or partitioning of the high-frequency spectrum into a finite number of areas as shown in Fig. 3.2. There are various methods of partitioning the spectrum. In one method described in Section 3.3, the spectrum is divided according to equal energy or areas. The center frequency of each area is assumed

to represent the frequency of the partition and the amplitude is taken as proportional to the square root of the area. For equal partitioning all sinusoids have the same amplitude. The approximate wave profile can be written as

$$H_W = \sum_{i=1}^{N} h_i \sin(\Omega_i t + \phi_i) \tag{3.1}$$

where H_W is the time-dependent wave amplitude about the mean water level, N is the number of discrete frequencies used to simulate the wave spectrum and h_i, Ω_i and ϕ_i are the amplitude, frequency and random phase of the ith sinusoid, respectively.

The number of sinusoids used to approximate the wave spectrum depends on the desired accuracy in simulating the wave spectrum density function chosen to model the actual waves. Because the chosen spectral density is itself modeled with only a given degree of accuracy, the benefit of using a large number of sinusoids to simulate the wave spectrum is questionable. Pakstys (Ref. 11) reports that some 20 randomly phased harmonic component waves used to simulate a sea spectrum resulted in wave statistics within one percent of those obtained directly from measurements of the sea. As soon as the frequency and amplitude for each partition have been selected, the wave forces can be obtained from precomputed distribution curves.

3.2. BRETSCHNEIDER SEA SPECTRUM

One of the most widely used sea spectrum descriptions is the Bretschneider Sea Spectrum, given by (Ref. 2)

$$S_w = \frac{A}{\Omega^5} e^{-B/\Omega^4} \tag{3.2}$$

where Ω the frequency of oscillation and

$$A = 2760\ H_S^2/T_S^4 \tag{3.3}$$

$$B = 690/T_S^4 \tag{3.4}$$

in which, H_S is the significant wave height and T_S is the average period of the significant waves. As stated in Sec. 2.3, H_S is the average of one-third highest waves (Ref. 2). Both H_S and T_S depend on the average wind speed. When the wind speed increases T_S increases, the lower end of the spectrum shifts towards the lower frequencies, as shown in Fig. (3.2). This may lead to resonance if the natural frequencies of the platform lie in the lower range.

3.3 DISCRETIZATION OF THE BRETSCHNEIDER SEA SPECTRUM

The energy contained between the frequencies $\Omega = \Omega$ and $\Omega = \infty$ is

$$E(\Omega) = \int_{\Omega}^{\infty} S_w(\Omega)d\Omega \qquad = \frac{A}{4B}\left[1 - \exp(-B/\Omega^4)\right] \tag{3.5}$$

Substituting Eqs. (3.3) and (3.4) into (3.5) we have

$$E(\Omega) = H_S^2[1 - \exp\ (-690/\Omega^4 T_S^4)] \tag{3.6}$$

When $\Omega = 0$, $E = E(0) = H_S^2$. If the wave spectrum is divided into M equal segments, then the energy E_i contained between Ω_{ui} the upper frequency of the segment and the

$\Omega = \infty$ is given by

$$E_i = E[1 - \exp\ (-690/\Omega_{ui}^4 T_S^4)] \tag{3.7a}$$

From Eq. (3.7a)

$$\Omega_{ui} = \frac{1}{T_S}\left[\frac{690}{\ln(\frac{1}{1-E_i/E})}\right]^{1/4} \tag{3.7b}$$

Also

$$\frac{E_i}{E} = \frac{M - i}{M} \quad , \; i = 1,2,\ldots,M - 1 \tag{3.8}$$

where M is the number of equal parts into which the spectrum is divided. Substituting Eq. (3.8) in (3.7b), we obtain

$$\omega_{ui} = \frac{1}{T_S}\left[\frac{690}{\ln(\frac{M}{i})}\right]^{1/4} \quad i = 1,2,\ldots,M - 1 \tag{3.9}$$

If we wish to find the frequencies corresponding to one half of the energy of one segment, then

$$\frac{E_i}{E} = \frac{M - i}{M} + \frac{E/2M}{E} = \frac{2M - 2i + 1}{2M}, \; i = 1,2,\ldots,M \tag{3.10}$$

and Eq. (3.9) can be rewritten as

$$\omega_i = \frac{1}{T_S}\left[\frac{690}{\ln(\frac{2M}{2i-1})}\right]^{1/4} \tag{3.11}$$

For a fully developed sea,

$$T_S = 7.34 \surd \overline{H_S} \tag{3.12}$$

Introducing Eq. (3.12) into (3.11), we obtain

$$\omega_i = \frac{0.6984}{\surd \overline{H_S}} \ln(\frac{2M}{2i-1})^{-1/4} \tag{3.13}$$

The amplitude of the pure sinusoid is given by

$$h = h_i = H_S/\surd\overline{M/2} \tag{3.14}$$

3.4 CONCLUDING REMARKS

In this dissertation, we asssume that the wave force is the only environmental force. If we represent the vector of the estimated wave forces in the ith partition by $\underset{\sim}{X}^*_{ei}$, then the jth component can be

written as

$$X^*_{ei,j} = D_{i,j}h \sin(\Omega_i t + \phi_i + \rho_i),\ j = 1,2,\ldots,6 \tag{3.15}$$

where, $D_{i,j}$ is the amplitude normalized with respect to the wave amplitude h, ϕ_i is the phase shift, Ω_i is the selected frequency of excitation and ρ_i is the random phase shift.

The equation of motion for the ith partition can be written as,

$$\dot{\underset{\sim}{x}}_i(t) = A_i \underset{\sim}{x}_i(t) + \underset{\sim}{P}_{ei} + \underset{\sim}{P}_{ci} + \underset{\sim}{N}_i \tag{3.16}$$

where $\underset{\sim}{x}_i$ is the state vector, A_i the state matrix based on added mass and damping at the center frequency Ω_i, $\underset{\sim}{P}_{ei}$ the vector of estimated environmental forces, $\underset{\sim}{P}_{ci}$ the vector of control forces and $\underset{\sim}{N}_i$ the vector of unmodeled environmental forces. The subscript i will be dropped for the remainder of this dissertation and will be invoked only when necessary.

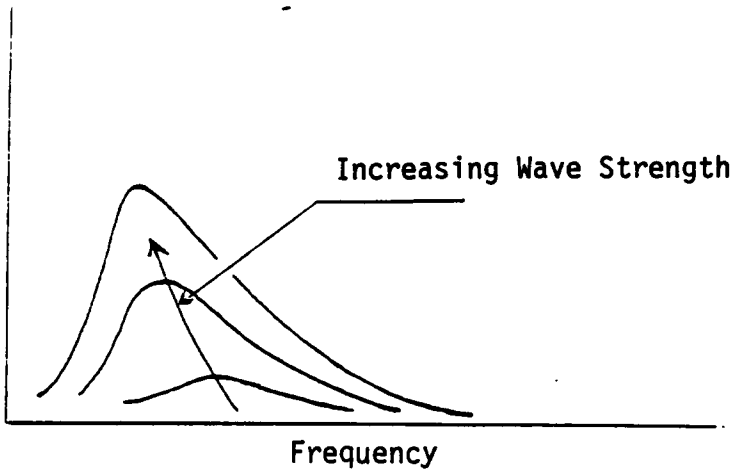

Fig. 3.1 - The Wave Spectrum

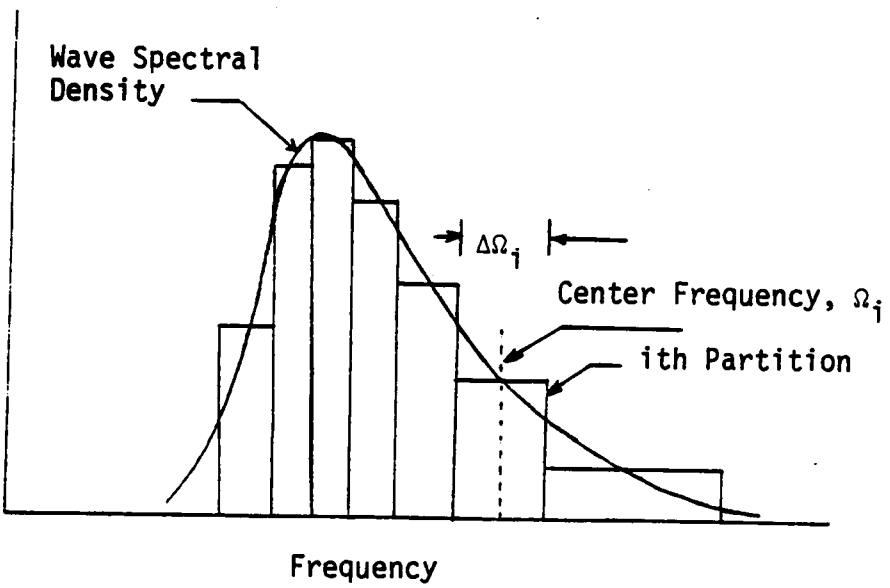

Fig. 3.2 - The Partitioned Wave Spectral Density

CHAPTER IV

ACTIVE VIBRATION CONTROL

4.1 INTRODUCTION

In Chapter 2 we derived the equations of motion of a semisubmersible structure (with a flexible superstructure) subjected to arbitrary excitation forces. It is well known that wave forces are random in nature and that wave heights are distributed in a Rayleigh distribution. The wave-induced motion of marine structures cause additional forces which depend on the velocity and acceleration of the structure. The coefficient matrix associated with the acceleration and velocity of the structure are known as added mass and added damping, respectively. Because these matrices depend on the frequency of oscillation of the wave, there is an infinite number of sets of state equations, one for each frequency in the continuous frequency spectrum. Because it is not possible to work with an infinite number of sets of state equations, it is necessary to discretize the frequency spectrum so that we have as many sets of state equations as increments. In Chapter 3, we presented a method of discretizing the spectrum by allocating the same amount of energy to each segment. The center frequency of each partition is used to calculate the mass and damping matrices of the corresponding segment by assuming that it remains constant within the segment. Also, the center frequency is used to estimate the phase and amplitude of the wave forces in each segment from precomputed distribution curves. The center frequency of a segment is defined to be the frequency corresponding to one half of the energy of

that segment. The actual excitation forces for a given segment can be regarded as a sum of the estimated forces and unmodeled forces. Moreover, the unmodeled forces can be regarded as random forces. The control forces are designed by the Independent Modal-Space Control (IMSC) method (Refs. 5-7). The responses computed for all the partitions can be added together to yield an estimate of the actual response. Because the estimated excitation forces modeled are only a deterministic approximation of the actual wave forces, the responses computed represent estimated values only. To improve the estimates it is necessary to use observers that take into account the difference in the measured responses and the estimated responses. The observers are designed such that the difference in the root mean square (RMS) values of the estimated and measured responses is brought down to an acceptable level. In this chapter, we first discuss the design of a controller for each segment. Then, we consider the problem of observer design. In Chapter 4, we present a numerical example demonstrating the technique.

4.2 THE EIGENVALUE PROBLEM AND DECOUPLING OF THE EQUATIONS OF MOTION

The eigenvalue problem can be derived by letting $\underset{\sim}{P}_e = \underset{\sim}{0}$ and $\underset{\sim}{P}_c = \underset{\sim}{0}$ in Eq. (2.44) and assuming a solution of the homogeneous problem in the exponential form

$$\underset{\sim}{x}(t) = e^{\lambda t}\underset{\sim}{x} \tag{4.1}$$

where λ and $\underset{\sim}{x}$ are constants, both quantities in general being complex. Canceling $e^{\lambda t}$ on both sides, we obtain the eigenvalue problem

$$A\underset{\sim}{x} = \lambda\underset{\sim}{x} \tag{4.2}$$

which has $2(6 + m)$ solutions λ_s, $\underset{\sim}{x}_s$, $(s = 1,2,\ldots,2(6 + m))$, where λ_s are the eigenvalues and $\underset{\sim}{x}_s$ are the associated eigenvectors.

To decouple the equations of motion, we must solve the adjoint eigenvalue problem

$$A^T\underset{\sim}{y} = \lambda\underset{\sim}{y} \tag{4.3}$$

It possesses the same eigenvalues λ_r but the set of left eigenvector $\underset{\sim}{y}_r$ is different from the set of right eigenvectors $\underset{\sim}{x}_s$. The two sets of eigenvectors are biorthogonal and can be normalized (Ref. 7) so as to satisfy

$$\underset{\sim}{y}_r^T\underset{\sim}{x}_s = 2\delta_{rs},\ \underset{\sim}{y}_r^TA\underset{\sim}{x}_s = 2\lambda_r\delta_{rs},\ r,s, = 1,2,\ldots,2(6 + m) \tag{4.4}$$

To formulate the problem in terms of real quantities, we assume p real eigenvalues and 2k complex eigenvalues. The complex eigenvalues and associated left and right eigenvectors occur in complex conjugate pairs. The eigevalues and eigenvectors can be written as

$$\underset{\sim}{x}_r = \underset{\sim}{a}_r,\ \underset{\sim}{y}_r = \underset{\sim}{c}_r,\ \lambda_r = \alpha_r,\ r = 1,2,\ldots,p \tag{4.5a,b,c}$$

$$\underset{\sim}{x}_r = \underset{\sim}{a}_r \pm i\underset{\sim}{b}_r,\ \underset{\sim}{y}_r = \underset{\sim}{c}_r \pm i\underset{\sim}{d}_r,\ \lambda_r = \alpha_r \pm i\omega_r,$$

$$r = p + 1,\ p + 2,\ldots,6 + m - p/2 \tag{4.5d,e,f}$$

Our objective is to formulate the problem in terms of real quantities alone. To this end, we can form the modal matrices (Ref. 7)

$$X = [\underset{\sim}{a}_1\ \ \underset{\sim}{a}_2\ \ \underset{\sim}{a}_3\cdots\underset{\sim}{a}_p\ \ \underset{\sim}{a}_{p+1}\ \ \underset{\sim}{b}_{p+1}\ \ \underset{\sim}{a}_{p+2}\ \ \underset{\sim}{b}_{p+2}$$

$$\cdots\underset{\sim}{a}_{6 + m - p/2}\ \ \underset{\sim}{b}_{6 + m - p/2}] \tag{4.6a}$$

$$Y = [\frac{1}{2}\underset{\sim}{c}_1\ \ \frac{1}{2}\underset{\sim}{c}_2\ \ \frac{1}{2}\underset{\sim}{c}_3\cdots\frac{1}{2}\underset{\sim}{c}_p\ \ \underset{\sim}{c}_{p+1},\ -\underset{\sim}{d}_{p+1}\ \ \underset{\sim}{c}_{p+2}\ -\underset{\sim}{d}_{p+2}$$

$$\cdots\underset{\sim}{c}_{6 + m - p/2}\ \ -\underset{\sim}{d}_{6 + m - p/2}] \tag{4.6b}$$

In terms of X and Y, the biorthonormality relations can be written as

$$Y^T X = I \quad , \quad Y^T A X = \Lambda \tag{4.7a,b}$$

where Λ is block-diagonal, in which

$$\Lambda_r = \alpha_r, \; r = 1,2,\ldots,p \tag{4.8a}$$

$$\Lambda_r = \begin{bmatrix} \alpha_r & \omega_r \\ -\omega_r & \alpha_r \end{bmatrix} , \; r = p+1, \; p+2,\ldots,6+m-p/2 \tag{4.8b}$$

Next, we introduce the linear transformation

$$\underset{\sim}{x} = X\underset{\sim}{z} \tag{4.9}$$

in Eq. (44), premultiply the resulting equation by Y^T and obtain

$$\dot{\underset{\sim}{z}} = \Lambda\underset{\sim}{z} + \underset{\sim}{Z} + \underset{\sim}{E} \tag{4.10}$$

where

$$\underset{\sim}{z}(t) = P^{-1}\underset{\sim}{x}^*(t) \tag{4.11a}$$

$$\underset{\sim}{Z} = Q^T\underset{\sim c}{X^*} \tag{4.11b}$$

$$\underset{\sim}{E} = Q^T\underset{\sim e}{X^*} \tag{4.11c}$$

in which

$$P = L^{-T}X \; , \; Q = L^{-T}Y \tag{4.12a,b}$$

If we write

$$z_r(t) = z_r(t) \; , \; r = 1,2,\ldots,p \tag{4.13}$$

and

$$\underset{\sim r}{z}(t) = [z_{2r-1}(t) \; z_{2r}(t)]^T \tag{4.14a}$$

$$\underset{\sim r}{Z} = [Z_{2r-1}(t) \; Z_{2r}(t)]^T \tag{4.14b}$$

$$\underset{\sim r}{E} = [E_{2r-1}(t) \; E_{2r}(t)]^T, \; r = p+1,p+2,\ldots,6+m-p/2 \tag{4.14c}$$

then Eq. (4.10) can be rewritten as

$$\dot{\underset{\sim}{z}}_r(t) = \Lambda_r \underset{\sim}{z}_r + \underset{\sim}{Z}_r + \underset{\sim}{E}_r, \quad r = 1,2,\ldots,p + k \tag{4.15}$$

where $\underset{\sim}{z}_r$, $\underset{\sim}{Z}_r$ and $\underset{\sim}{E}_r$ are vectors of modal displacements, modal control forces and modal excitation forces, respectively. If $\underset{\sim}{Z}_r \equiv \underset{\sim}{0}$, Eqs. (4.15) are independent. When $\underset{\sim}{Z}_r \neq \underset{\sim}{0}$, the modal control represents feedback control and has the general functional dependence

$$\underset{\sim}{Z}_r = \underset{\sim}{Z}_r (\underset{\sim}{z}_1, \underset{\sim}{z}_2,\ldots,\underset{\sim}{z}_{p+k}), \quad r = 1,2,\ldots,p + k \tag{4.16}$$

so that Eqs. (45.1) are coupled through the control forces. In such a case, we refer to Eqs. (4.15) as internally (plant) decoupled but externally (controller) coupled. In the special case in which the modal control $\underset{\sim}{Z}_r$ depends on $\underset{\sim}{z}_r$ alone

$$\underset{\sim}{Z}_r = \underset{\sim}{Z}_r(\underset{\sim}{z}_r), \quad r = 1,2,\ldots,p + k \tag{4.17}$$

Eqs. (4.15) represent uncoupled pairs of first order differential equations. In the following, we assume that this is the case and use Eqs. (4.15) to design control forces in the modal space.

4.3 OPTIMAL CONTROL IN MODAL SPACE

Usually, the mass of the flexible superstructure is much smaller than the mass of the rigid platform. In such cases, the displacements of the rigid platform affect the elastic motion of the flexible structure, but the effect of the flexible structure on the rigid platform is sufficiently small that it can be ignored. Also, damped modes are primarily associated with the motion of the rigid platform and undamped modes are primarily associated with the motion of the flexible structure. To reflect the damped motion of the rigid platform and undamped elastic motion of the flexible structure, we can partition the

modal state vector and the associated control vector and excitation vector as follows:

$$\underset{\sim}{z} = [\underset{\sim}{z}_1^T \ \underset{\sim}{z}_2^T]^T \ , \quad \underset{\sim}{Z} = [\underset{\sim}{Z}_1^T \ \underset{\sim}{Z}_2^T]^T \ , \quad \underset{\sim}{E} = [\underset{\sim}{E}_1^T \ \underset{\sim}{E}_2]^T \qquad (4.18a,b,c)$$

where the subscripts 1 and 2 correspond to modes associated with the displacements of the rigid structure and elastic displacements of the flexible structure, respectively. Similarly, we can partition the coefficient matrix Λ as follows:

$$\Lambda = \left[\begin{array}{c|c} \Lambda_1 & 0 \\ \hline 0 & \Lambda_2 \end{array}\right] \qquad (4.19)$$

where Λ_1 is a 12×12 matrix corresponding to the modes associated with the motion of the rigid platform and Λ_2 is a 2m×2m matrix corresponding to the elastic modes associated with the motion of the flexible structure. The transformation matrix P can also be partitioned in the form

$$P = \left[\begin{array}{c|c} P_{11} & P_{12} \\ \hline P_{21} & P_{22} \\ \hline P_{31} & P_{32} \\ \hline P_{41} & P_{42} \end{array}\right] \qquad (4.20)$$

where P_{11} and P_{31} are 12×12 submatrices representing the contribution of the modes associated with the motion of the rigid platform to the velocities and displacements of the rigid platform, respectively. The entries in P_{12} and P_{32} must be regarded as negligible compared to the entries in P_{11} and P_{31}, consistent with the assumption that the mass of the flexible structure is much smaller than the mass of the rigid

platform. Submatrices P_{21} and P_{41} represent the contribution of the modes associated with the motion of the rigid platform to the elastic velocities and displacements, respectively. Finally, P_{22} and P_{42} represent the contribution of the modes associated with the motion of the flexible structure to the elastic velocities and displacements, respectively.

It can be shown that (Ref. 7) submatrices P_{31}, P_{32}, P_{41}, P_{42} must satisfy the relationships

$$P_{31}\underset{\sim}{Z}_1 + P_{32}\underset{\sim}{Z}_2 = \underset{\sim}{0}\ , \quad P_{41}\underset{\sim}{Z}_1 + P_{42}\underset{\sim}{Z}_2 = \underset{\sim}{0} \tag{4.21a,b}$$

Because the entries in P_{32} can be ignored compared to the entries in P_{31}, we have

$$P_{31}\underset{\sim}{Z}_1 = \underset{\sim}{0} \tag{4.22}$$

Also, the columns of P_{42} occur as interdependent pairs (Ref. 4) corresponding to an undamped system. Hence, we have

$$P_{42}\underset{\sim}{Z}_2 = \underset{\sim}{0} \tag{4.23}$$

Let us further split the vectors $\underset{\sim}{Z}_1$ and $\underset{\sim}{Z}_2$ into controlled and uncontrolled parts, so that

$$\underset{\sim}{Z}_1 = [\underset{\sim}{Z}_{1C}^T \ \ \underset{\sim}{Z}_{1R}^T]^T\ , \quad \underset{\sim}{Z}_2 = [\underset{\sim}{Z}_{2C}^T \ \ \underset{\sim}{Z}_{2R}]^T \tag{4.24a,b}$$

where the subscripts C and R refer to controlled and residual quantities, respectively. For the modes associated with the motion of the rigid platform, we can write P_{31} as

$$P_{31} = [P_{11}^* \ \ P_{12}^*] \tag{4.25}$$

where P_{11}^* and P_{12}^* correspond to controlled and uncontrolled modes, respectively. Then, according to Eq. (4.22) we have

$$P_{11}^*\underset{\sim}{Z}_{1C} + P_{12}^*\underset{\sim}{Z}_{1R} = \underset{\sim}{0} \tag{4.26a}$$

from which it follows that

$$\underset{\sim}{Z}_{1R} = -(P^*_{12})^{-1}P^*_{11}\underset{\sim}{Z}_{1C} \tag{4.26b}$$

Equation (4.26b) implies that only one half of the damped modes associated with the displacements of the rigid platform can be controlled independently. The same conclusion was reached in other investigations (Ref. 7). In certain cases, displacements and velocities of the rigid platform can be independent of each other, or the dependence can be extremely weak. For example, the coupling between surge and pitch motions is often negligible. In such cases P^*_{11} and P^*_{12} contain zero rows and Eq. (4.26b) is no longer valid. This implies that each mode associated with the motion of the rigid platform, can be controlled independently. Moreover, if z_i and z_j are two modal displacements corresponding to two different real eigenvalues and contributing to the same displacement of the rigid structure, then it follows from Eq. (4.22) that Z_i and Z_j can take the form

$$K_iZ_i + K_jZ_j = 0 \tag{4.27}$$

where K_i and K_j are two elements belonging to P_{31}. Equation (4.27) can be regarded as a constraint equation implying that only one half of the modal displacements associated with real eigenvalues can be controlled independently. In this dissertation we assume that this is the case.

Next, we observe from Eq. (4.23) that any number of modes associated with the motion of the flexible structure can be controlled. Because the lower modes require less energy to excite than higher modes, we consider controlling the lower modes only. To this end, we consider proportional control, so that the control vector can be expressed in terms of the modal state vector as follows:

$$\underset{\sim}{Z} = G\underset{\sim}{z} \tag{4.28}$$

where G is the modal gain matrix, which can be expressed in the partitioned form

$$G = \begin{bmatrix} G_C & 0 \\ 0 & 0 \end{bmatrix} \tag{4.29}$$

If we assume that all the rigid modes are controlled, then the modal equations can be written as

$$\begin{bmatrix} \dot{\underset{\sim}{z}}_C \\ \dot{\underset{\sim}{z}}_R \end{bmatrix} = \begin{bmatrix} \Lambda_C + G_C & 0 \\ 0 & 0 \end{bmatrix} \begin{bmatrix} \underset{\sim}{z}_C \\ \underset{\sim}{z}_R \end{bmatrix} + \begin{bmatrix} \underset{\sim}{E}_C \\ \underset{\sim}{E}_R \end{bmatrix} \tag{4.30}$$

If the modal control force $\underset{\sim}{Z}_{C,r}$ is a function of $\underset{\sim}{z}_r(t)$ alone, then G_C has the block-diagonal form

$$G_C = \text{block-diag } G_r \tag{4.31}$$

If we consider controlling all the modes with real eigenvalues and the first n modes corresponding to the complex eigenvalues, then we have

$$G_r = 0, \quad G_{r+p/2} = G_{r+p/2}, \quad r = 1,2,\ldots,p/2 \tag{4.32a,b}$$

$$G_r = \begin{bmatrix} G_{r11} & G_{r12} \\ G_{r21} & G_{r22} \end{bmatrix}, \quad r = p+1,\ p+2,\ldots,p+n \tag{4.32c}$$

For optimal control, G can be determined by minimizing a cost function of the form

$$J = \sum_{r=1}^{p/2} J_r^* + \sum_{r=p+1}^{p+n} J_r \tag{4.33}$$

where J_r^* and J_r are modal cost functions. Because each mode is controlled independently, the modal cost functions J_r^* and J_r are independent of one another. It then follows that J can be minimized by

minimizing each J_r^* and J_r independently. The modal cost functions J_r^* and J_r are assumed to have the form

$$J_r^* = \int_0^{t_f} [z_r^2 Q_r^* + Z_r^2 R_r^*]dt \quad r = 1,2,\ldots,p/2 \tag{4.34a}$$

$$J_r = \int_0^{t_f} [\underset{\sim}{z}_r^T Q_r \underset{\sim}{z}_r + \underset{\sim}{Z}_r^T R_r \underset{\sim}{Z}_r]dt \ , \ r = p+1, p+2,\ldots p+n \tag{4.34b}$$

where Q_r^* is a nonnegative number, R_r^* is a positive number, Q_r is a positive semidefinite matrix and R_r is a positive definite matrix. For simplicity, we assume that $Q_r^* = 1$ and $Q_r = I$, so that

$$J_r^* = \int_0^{t_f} [z_r^2 + Z_r^2 R_r^*]dt, \ r = 1,2,\ldots,p/2 \tag{4.35a}$$

$$J_r = \int_0^{t_f} [\underset{\sim}{z}_r^T \underset{\sim}{z}_r + \underset{\sim}{Z}_r^T R_r \underset{\sim}{Z}_r]dt, \ r = p+1, p+2,\ldots,p+n \tag{4.35b}$$

This leaves us with the problem of selecting R_r^* and R.

It is shown in Ref. 8 that the optimal control gain matrix has the form

$$G_r(t) = -(R_r^*)^{-1} K_r^*(t), \ r = 1,2,\ldots,p/2 \tag{4.36a}$$

$$G_r(t) = -R_r^{-1} K_r(t), \ r = p+1, p+2,\ldots,p+n \tag{4.36b}$$

where $K_r^*(t)$ is a real variable satisfying the Riccati equation

$$\dot{K}_r^*(t) = -2\alpha_{r+p/2} K_r^*(t) - 1 + (R_r^*)^{-1} K_r^{*2}, \ K_r^*(t_f) = 0,$$

$$r = 1,2,\ldots,p/2 \tag{4.37a,b}$$

and $K_r(t)$ is a real symmetric matrix satisfying the Ricatti equation

$$\dot{K}_r(t) = -K_r(t)\Lambda_r - \Lambda_r^T K_r(t) - I + K_r(t) R_r^{-1} K_r(t), \ K_r(t_f) = 0,$$

$$r = p+1, p+2,\ldots,p+n \tag{4.37c,d}$$

The weighting factor R_r^* is a mere scalar. On the other hand, R_r is a matrix, which on physical grounds can be chosen in the form (Ref. 7)

$$R_r = \begin{bmatrix} \infty & 0 \\ 0 & R_{r22} \end{bmatrix}, \quad r = p + 1,\ p + 2,\ldots,p + n \tag{4.38}$$

from which it follows that

$$R_r^{-1} = \begin{bmatrix} 0 & 0 \\ 0 & R_{r22}^{-1} \end{bmatrix}, \quad r = p + 1,\ p + 2,\ldots,p + n \tag{4.39}$$

Hence, $\underset{\sim}{Z}_r$ can be written as

$$\underset{\sim}{Z}_r = \begin{bmatrix} 0 \\ -R_{r22}^{-1}(K_{r21}z_{2r-1} + K_{r22}z_{2r}) \end{bmatrix}, \quad r = p + 1,\ p + 2,\ldots,p + n \tag{4.40}$$

As soon as a value for R_{r22} has been chosen, we can solve the scalar equations

$$\begin{aligned} \dot{K}_{r11} &= -2\alpha_r K_{r11} + 2\omega_r K_{r12} - 1 + R_{r22}^{-1}K_{r12}^2 \\ \dot{K}_{r12} &= -\omega_r K_{r11} - 2\alpha_r K_{r12} + \omega_r K_{r22} + R_{r22}^{-1}K_{r12}K_{r22} \\ \dot{K}_{r22} &= -2\omega_r K_{r11} - 2\alpha_r K_{r12} - 1 + R_{r22}^{-1}K_{r22}^2, \end{aligned}$$

$$r = p + 1,\ p + 2,\ldots,p + n \tag{4.41}$$

It is shown in Ref. 8 that if Q_r^* and R_r^* are the constant scalars and Q_r and R_r are constant matrices, then as $t_f \to \infty$, $K_r^*(t) \to K_r^* = \text{const}$ and $K_r(t) \to K_r = \text{const}$, which implies that $\dot{K}_r^*(t) \to 0$ and $\dot{K}_r(t) \to 0$.

In this paper, we assume that t_f is sufficiently large that steady-state

solution of the Riccati equations can be used. Hence, Eq. (4.37a) yields

$$K_r^* = \frac{\alpha_{r+p/2} \pm \sqrt{\alpha_{r+p/2}^2 + (R_r^*)^{-1}}}{(R_r^*)^{-1}} \tag{4.42}$$

and the steady-state value of K_r can be obtained from Eqs. (4.41). For undamped systems, Eqs. (4.41) admit a closed-form steady-state solution (Ref. 4)

$$K_{12} = K_{21} = -\omega_r R_{r22} + \sqrt{\omega_r^2 R_{r22}^2 + R_{r22}} \tag{4.43a}$$

$$K_{22} = (R_{r22} - 2\omega_r^2 R_{r22}^2 + 2\omega_r R_{r22} \sqrt{\omega_r^2 R_{r22}^2 + R_{r22}})^{1/2} \tag{4.43b}$$

$$K_{11} = [\omega_r^{-2} + 2\omega_r^{-1} R_{r22}^{-1}(\omega_r^2 R_{r22}^2 + R_{r22})^{3/2} - 2R_{r22}^2 \omega_r^2 - R_{r22}]^{1/2} \tag{4.43c}$$

For damped systems the steady-state solution can be computed by Potter's method (Ref. 13)

At this point we can appreciate the benefit derived from the IMSC method. The general coupled control method involves a large order Riccati equation. For high-order systems (> 40) this can present severe computational difficulties. If the IMSC method is used, then it is necessary to solve sets of independent first-order or second-order Riccati equations, instead of solving a single matrix Riccati equation of high order.

To select the values of R_r^* and R_{r22}, we return to the closed-loop equation, Eq. (4.30). Inserting Eqs. (4.40) and (4.36) into (4.30), we obtain

$$\dot{z}_r = \alpha_r z_r + E_r$$

$$\dot{z}_{r+p/2} = -(\sqrt{\alpha^2_{r+p/2} + (R^*_r)^{-1}})z_{r+p/2} + E_{r+p/2},\ r = 1,2,\ldots,p/2 \quad (4.44a,b)$$

$$\dot{\underset{\sim}{z}}_r = \Lambda^*_r \underset{\sim}{z}_r + E_r,\ r = p+1,\ p+2,\ldots,p+n \quad (4.44c)$$

where Λ^*_r are nonsymmetric matrices given by

$$\Lambda^*_r = \begin{bmatrix} \alpha_r & \omega_r \\ -(\omega_r + R^{-1}_{r22}K_{r21}) & \alpha_r - R^{-1}_{r22}K_{r22} \end{bmatrix} \quad (4.45)$$

Letting

$$z_{r+p/2} = e^{\lambda^*_{r+p/2}t} z^*_{r+p/2},\ r = 1,2,\ldots,p/2 \quad (4.46a)$$

$$\underset{\sim}{z}_r = e^{\lambda^*_r t}\underset{\sim}{z}^*_r,\ r = p+1,\ p+2,\ldots p+n \quad (4.46b)$$

we obtain the eigenvalue problems

$$-(\sqrt{\alpha^2_{r+p/2} + (R^*_r)^{-1}})z_{r+p/2} = \lambda^*_{r+p/2}z_{r+p/2},\ r = 1,2,\ldots,p/2 \quad (4.47a)$$

$$\Lambda^*_r \underset{\sim}{z}_r = \lambda^*_r \underset{\sim}{z}_r,\ r = p+1,\ p+2,\ldots,p+n \quad (4.47b)$$

Then, R^*_r can be obtained from

$$\lambda^*_{r+p/2} = -\sqrt{\alpha^2_{r+p/2} + (R^*_r)^{-1}} \quad (4.48)$$

where $\lambda^*_{r+p/2}$ is a preselected closed-loop eigenvalue corresponding to a real open-loop eigenvalue $\alpha_{r+p/2}$. Finally, R_{r22} is selected such that the eigenvalue of Λ^*_r lies to the left of its open-loop counterpart. As soon as R^*_r and R_r have been determined, the modal gain matrices can be written as

$$G_r = -(\alpha_{r+p/2} + \sqrt{\alpha^2_{r+p/2} + (R^*_r)^{-1}}) \quad r = 1,2,\ldots,p/2 \quad (4.49a)$$

$$G_r = -R^{-1}_{r22}\begin{bmatrix} 0 & 0 \\ K_{r12} & K_{r22} \end{bmatrix} r = p+1,\ p+2,\ldots,p+n \quad (4.49b)$$

Then, the contol force vector $\underset{\sim}{Z}_r$ can be determined by

$$\underset{\sim}{Z}_r = G_r \underset{\sim}{z}_r(t) \tag{4.50}$$

Finally, the actual control force $\underset{\sim}{X}^*_C(t)$ and response $\underset{\sim}{x}^*(t)$ can be found by using the transformation

$$\underset{\sim}{X}^*_C(t) = LY^{-T}\underset{\sim}{Z}(t) \tag{4.51}$$

$$\underset{\sim}{x}^*(t) = L^{-T}X\underset{\sim}{z}(t) \tag{4.52}$$

4.4 DESIGN OF OBSERVERS

Until now the discussion has been confined to the generation of control and to the estimation of the states after estimating the wave forces in each partition. The estimated states are likely to be different from the actual states because the exact wave forces are not known. To narrow the difference between the actual states and the estimated states, it is necessary to design an observer for each partition in the wave spectrum.

The task of the observer is to extract the state vector $\underset{\sim}{z}$ from the system output. However, the output $\underset{\sim}{w}_i$, obtained by filtering the total output through a filter of bandwidth $\Delta\Omega_i$ (Fig. 4), contains contributions not only from the frequency Ω_i but also from the other frequencies in the partition.

The actual system can be written in the modal form

$$\dot{\underset{\sim}{z}}_i = \Lambda_i \underset{\sim}{z}_i + G_i \underset{\sim}{z}_i + Y_i^T L_i^{-1} \underset{\sim}{F}_{e,i} + Y_i^T L_i^{-1} \underset{\sim}{N}_i \tag{4.53}$$

where $\underset{\sim}{F}_{e,i}$ is the estimated excitation force in the ith interval and $\underset{\sim}{N}_i$ is the vector of unmodeled disturbances. The measurement vector $\underset{\sim}{w}_i$ can be expressed as

$$\underset{\sim}{w}_i = C_i^* \underset{\sim}{z}_i + \underset{\sim}{\gamma}_i \tag{4.54}$$

where

$$C_i^* = C_i L_i^{-T} X_i \tag{4.55}$$

in which C_i is the $\ell \times 2(6 + m)$ measurement matrix, $\ell < 2(6 + m)$ implying that the measurement vector $\underset{\sim}{w}_i$ is not complete, and $\underset{\sim}{\gamma}_i$ is the error vector stemming from the fact that Λ_i, which actually varies with the frequency of oscillation, is assumed remain constant within each partition.

Our objective is to construct an observer to improve the estimate of the state vector $\underset{\sim}{z}$. Observers are dynamical systems similar to the actual system and having as input the output of the actual system. The observer eigenvalues are chosen such that the differences in the root-mean-square (RMS) values of the actual measurements and the estimated measurements are brought down to an acceptable level. We choose the observer in the form

$$\begin{bmatrix} \dot{\hat{\underset{\sim}{z}}}_{Ci}(t) \\ \hline \dot{\hat{\underset{\sim}{z}}}_{Ri}(t) \end{bmatrix} = \left[\begin{array}{c|c} \Lambda_{Ci} & 0 \\ \hline 0 & \Lambda_{Ri} \end{array}\right] \begin{bmatrix} \hat{\underset{\sim}{z}}_{Ci} \\ \hline \underset{\sim}{z}_{Ri} \end{bmatrix} + G_i \begin{bmatrix} \hat{\underset{\sim}{z}}_{Ci} \\ \hline \underset{\sim}{z}_{Ri} \end{bmatrix} + Y_i^T L_i^{-1} \underset{\sim}{F}_{e,i} + \mu_i (\underset{\sim}{w}_i - \hat{\underset{\sim}{w}}_i) \tag{4.56}$$

where

$$\hat{\underset{\sim}{w}}_i = C_i^* \hat{\underset{\sim}{z}}_i \tag{4.57}$$

Next, we introduce the error vector

$$\underset{\sim}{\varepsilon}_i = \hat{\underset{\sim}{z}}_i - \underset{\sim}{z}_i \tag{4.58}$$

Inserting $G_i \underset{\sim}{z}_i = G_i \hat{\underset{\sim}{z}}_i$ in Eq. (4.53), we have

$$\dot{\underset{\sim}{z}}_i = \Lambda_i \underset{\sim}{z}_i + G_i \underset{\sim}{z}_i + G \underset{\sim}{\varepsilon}_i + Y_i^T L_i^{-1} (\underset{\sim}{F}_{e,i} + \underset{\sim}{N}_i) \tag{4.59}$$

Subtracting Eq. (4.59) from (4.56), and combining the resulting equation with Eq. (4.59) we have

$$\begin{bmatrix} \dot{z}_{Ci} \\ \dot{z}_{Ri} \\ \dot{\varepsilon}_{Ci} \\ \dot{\varepsilon}_{Ri} \end{bmatrix} = \left[\begin{array}{c|c|c|c} \Lambda_{Ci} + G_{Ci} & 0 & G_{Ci} & 0 \\ \hline 0 & \Lambda_{Ri} & 0 & 0 \\ \hline 0 & 0 & \Lambda_{Ci} - \mu_{Ci}C^*_{Ci} & -\mu_{Ci}C^*_{Ri} \\ \hline 0 & 0 & -\mu_{Ri}C^*_{Ci} & \Lambda_{Ri} - \mu_{Ri}C^*_{Ri} \end{array}\right] \begin{bmatrix} z_{Ci} \\ z_{Ri} \\ \varepsilon_{Ci} \\ \varepsilon_{Ri} \end{bmatrix} + \left[\begin{array}{c} Y_i^T L^{-L}(F_{e,i} + N_i) \\ \hline -Y_i^T L^{-1} N_i + \mu_i Y_i \end{array}\right] \tag{4.60}$$

Inspection of Eq. (4.60) shows that the system eigenvalues can be designed separately in accordance with the deterministic separation principle (Ref. 4). Inspection of Eq. (4.60) also shows that spillover from residual modes as represented by $\mu_{Ci}C^*_{Ri}$ exists. This spillover will not destabilize the system if the observer gains are chosen properly.

4.5 DISCRETE-TIME SOLUTIONS

Numerical simulations and on board computations are carried out most efficiently on digital computers. Moreover, it is practical to make measurements at preselected time intervals. This makes it necessary to seek a discrete-time solution. The process of discretization in time transforms the first-order differential equations into

difference equations. After dropping the subscript i, the dynamical equation for the observer, Eq. (4.56), can be rewritten as

$$\begin{bmatrix} \hat{z}_C(t) \\ \hat{z}_R(t) \end{bmatrix} = \left[\begin{array}{c|c} \Lambda_C + G_C & 0 \\ \hline 0 & 0 \end{array}\right] \begin{bmatrix} \hat{z}_C \\ \hat{z}_R \end{bmatrix} + \underset{\sim}{E} + \underset{\sim}{M} \tag{4.61}$$

where

$$\underset{\sim}{E} = Y^T L^{-1} \underset{\sim}{F}_e \ , \quad \underset{\sim}{M} = \mu(\hat{\underset{\sim}{w}} - \hat{\underset{\sim}{w}}) \tag{4.62a,b}$$

In Section 4.3, we saw that the IMSC approach leads to a block-diagonal form for G_c and the resulting modal equations are both internally and externally decoupled. Following Eqs. (4.44), we write the modal equations for the observer

$$\dot{\hat{z}}_r(t) = \alpha_r \hat{z}_r(t) + E_r + M_r, \tag{4.63a}$$

$$\dot{\hat{z}}_{r+p/2}(t) = -(\sqrt{\alpha^2_{r+p/2} + (R^*_r)^{-1}}\ \hat{z}_{r+p/2}(t) + E_{r+p/2} + M_{r+p/2},$$

$$r = 1,2,\ldots,p/2 \tag{4.63b}$$

$$\dot{\hat{\underset{\sim}{z}}}_r(t) = \Lambda^*_r \hat{z}_{r+p/2}(t) + \underset{\sim}{E}_r + \underset{\sim}{M}_r, \quad r = p+1, p+2,\ldots,p+n \tag{4.63c}$$

$$\dot{\hat{\underset{\sim}{z}}}_r(t) = \Lambda_r \hat{\underset{\sim}{z}}_r(t) + \underset{\sim}{E}_r + \underset{\sim}{M}_r, \quad r = p+n+1, p+n+2,\ldots,p+k \tag{4.63d}$$

where Λ^*_r, Λ_r are given by Eqs. (4.45) and (4.8b), respectively. Moreover, $\underset{\sim}{E}_r$ and $\underset{\sim}{M}_r$ the estimated modal excitation and the correction term for unmodeled excitation forces, respectively. If T is the samping interval, the discrete-time solution of Eqs. (4.63) is given by (Ref. 10)

$$\hat{z}_r(K+1) = (1 + \lambda_r T)\hat{z}_r(K) + [E_r(K) + M_r(K)]T, \quad r = 1,2,\ldots,p/2 \tag{4.64a}$$

$$\hat{z}_{r+p/2}(K+1) = (1 + \lambda_{r+p/2}T)\hat{z}_{r+p/2}(K) + [E_{r+p/2}(K) + M_{r+p/2}(K)]T,$$

$$r = 1,2,\ldots,p/2 \quad (4.64b)$$

$$\hat{\underset{\sim}{z}}_r(K+1) = \Phi^*_r\hat{\underset{\sim}{z}}_r(K) + \Gamma^*_r[\underset{\sim}{E}_r(K) + \underset{\sim}{M}_r(K)],\ r = p+1,\ p+2,\ldots,p+n \quad (4.64c)$$

$$\hat{\underset{\sim}{z}}_r(K+1) = \Phi_r\hat{\underset{\sim}{z}}_r(K) + \Gamma_r[\underset{\sim}{E}_r(K) + \underset{\sim}{M}_r(K)],$$

$$r = p+n+1,\ p+n+2,\ldots,p+k \quad (4.64d)$$

where

$$\Phi^*_r = e^{\Lambda^*_r T} = I + T\Lambda^*_r + \frac{T^2}{2!}\Lambda^{*2}_r + \frac{T^3}{3!}\Lambda^{*3} + \ldots . \quad (4.65a)$$

$$\Gamma^*_r = \int_0^T e^{t\Lambda^*_r}dt = [\Phi^*_r - I](\Lambda^*_r)^{-1} \quad (4.65b)$$

$$\Phi_r = e^{\Lambda_r T} = I + T\Lambda_r + \frac{T^2}{2!}\Lambda^2_r - \frac{T^3}{3!}\Lambda^3_r + \ldots . \quad (4.65c)$$

$$\Gamma_r = \Gamma\int_0^T e^{t\Lambda_r}dt = [\Phi_r - I]\Lambda_r^{-1} \quad (4.65d)$$

The solution of the discrete time difference equations is stable when the eigenvalues of Φ^*_r and Φ_r lie inside a unit circle (Ref. 10). This can be achieved by choosing T sufficiently small.

CHAPTER V

NUMERICAL EXAMPLE

5.1 MATHEMATICAL MODEL

We now demonstrate the control technique outlined in Chapter 4 by means of a numerical example. A circular platform is considered because the angle of incidence of the environmental disturbance may vary over a wide range. The flexible superstructure is chosen in the form of a cantilever beam attached to the platform. The dimensions of the platform and its hydrodynamic characteristics are as in Ref. 12. An illustration of the structure is shown in Fig. 5.1 and its dimensions are given in Table 5.1. The body-fixed system of coordinates is shown in Fig. 5.2. It is assumed that the structure is exposed to waves with significant height of 4m.

For small motions, the linearized hydrodynamic stiffness coefficients are given by

$$k_{Rxx} = k_{Ryy} = 0,\ k_{Rzz} = 8.24\times10^{6}\ \text{N/m}$$

$$k_{R\phi\phi} = k_{R\psi\psi} = 3.1\times10^{9}\ \text{N/rad},\ k_{R\nu\nu} = 0$$

The distribution of potential damping as a function of frequency of oscillation Ω (shown in Figs. 5.3 - 5.6) is given approximately by

$$C_{axx} = 2.78\ (\Omega - 0.3)10^{8} \text{ for } \Omega > 0.3 \tag{5.1a}$$

$$C_{a\psi\psi} = 13.88\ (\Omega - 0.3)^{2}10^{10} \text{ for } \Omega > 0.3 \tag{5.1b}$$

$$C_{ax\psi} = C_{a\psi x} = 8.5\ (\Omega - 0.3)^{2}10^{9} \text{ for } \Omega > 0.3 \tag{5.1c}$$

Although in general added mass terms vary with the frequency, for relatively small frequencies, such as those considered in this example,

they remain constant. The added mass terms are

$$M_{axx} = M_{ayy} = 1.1\times10^{8}\ N/(m/s^2),\ M_{azz} = 5.9\times10^{7}\ N/(m/s^2)$$

$$M_{a\phi\phi} = M_{a\psi\psi} = 2.63\times10^{10}\ N\cdot m/(rad/s^2),\ M_{ax\psi} = M_{ay\phi} = 2.6\times10^{8}\ N/(rad/s^2)$$

$$M_{a\psi x} = M_{a\phi y} = 2.6\times10^{8}\ N\cdot m/(m/s^2)$$

The distribution of the amplitude of excitation forces as a function of the frequency of oscillation Ω (shown in Figs. 5.7 - 5.8) is given approximately by

$$F_{ex} = (5.82 - 1.64\ \Omega^2)h_w \text{ for } \Omega \le 0.5 \qquad (5.2a)$$

$$F_{ex} = (2.69 - 5.26\ (\Omega - 0.69)^2)10^7 h_w \text{ for } \Omega > 0.5 \qquad (5.2b)$$

$$M_{\psi} = (11\Omega^2 - 6\Omega^3)10^8 h_w \qquad (5.2c)$$

where h_w is the wave aplitude. We consider only two degrees of freedom for the rigid-body motion: the longitudinal motion x and the pitching motion ψ. The wave spectrum was partitioned into six segments of equal energy, and the second segment with center frequency of 0.32181 rad/s was used. The cantilever was divided into four finite elements with 2 degrees of freedom for each node, as shown in Fig. 5.2. The resulting system had 10 degrees of freedom: 2 for the rigid platform and 8 for the flexible structure.

5.2 THE FINITE ELEMENT MODEL OF THE FLEXIBLE CANTILEVER BEAM

Figure 5.2 shows the nodal locations and the element numbers. Figure 5.9 shows the nodal locations for a typical element where ζ is the local coordinate along the axis of the cantilever and h is the length of the element. Hermite cubics are chosen as the interpolation

functions. The displacement $u_x^{(i)}(z^*)$ for the ith element is given by

$$u_x^{(i)}(z^*) = Lq_i \tag{5.3}$$

where

$$L = [L_1 \quad hL_2 \quad L_3 \quad hL_4] \tag{5.4a}$$

is the row matrix of interpolating functions, where

$$L_1 = 3\zeta^2 - 2\zeta^3 \tag{5.4b}$$

$$L_2 = \zeta^2 - \zeta^3 \tag{5.4c}$$

$$L_3 = 1 - 3\zeta^2 + 2\zeta^3 \tag{5.4d}$$

$$L_4 = -\zeta + 2\zeta^2 - \zeta^3 \tag{5.4e}$$

in which

$$\zeta = (n - i + 1) - z^*/h \tag{5.4f}$$

where n is the number of equal length elements of the cantilever. In the present case n = 4.

Moreover, q_i is the vector of nodal displacements given by

$$q_i = [q_{4(i-1)+1} \; q_{4(i-1)+2} \; q_{4(i-1)+3} \; q_{4(i-1)+4}]^T \tag{5.5}$$

The matrix of direction cosines is

$$R_i = I \tag{5.6}$$

From Eq. (2.11b),

$$\phi_i = \int_{m_i} LR_i dm_i \tag{5.7}$$

Considering Figs. (5.4) and (5.5), using Eq. (5.7) and carrying out the necessary integrations, we obtain

$$\phi_i = [\tfrac{1}{2}\rho h \quad \tfrac{1}{12}\rho h^2 \quad \tfrac{1}{2}\rho h \quad -\tfrac{1}{12}\rho h^2] \tag{5.8}$$

where ρ is the mass per unit length of the cantilever and h is the length of an element. From Eq. (2.11b),

$$\bar{\phi}_i = \int_{m_i} R_i L^T L R_i dm_i \tag{5.9}$$

Inserting Eqs. (5.4) - (5.6) into Eq. (5.9), we have

$$\bar{\phi}_i = - \rho h \int_1^0 L^T L d\zeta \tag{5.10}$$

where

$$L^T L = \begin{bmatrix} L_1^2 & & & \\ hL_1L_2 & hL_2^2 & & \text{Symm} \\ L_1L_3 & hL_2L_3 & L_3^2 & \\ hL_1L_4 & h^2L_2L_4 & hL_3L_4 & h^2L_4^2 \end{bmatrix} \tag{5.11}$$

Carrying out the integrations, we obtain

$$\bar{\phi}_i = \begin{bmatrix} \frac{13}{35}\rho h & & & \\ \frac{11}{210}\rho h^2 & \frac{1}{105}\rho h^3 & & \text{Symm} \\ \frac{9}{70}\rho h & \frac{13}{420}\rho h^2 & \frac{3}{5}\rho h & \\ \frac{-13}{420}\rho h^2 & \frac{-1}{140}\rho h^2 & \frac{-11}{210}\rho h^2 & \frac{1}{105}\rho h^3 \end{bmatrix} \tag{5.12}$$

From Eq. (2.21b), we have

$$\tilde{\phi}_i^T = \int_{m_i} R_i L_i^T (\tilde{r}_E + \tilde{\varrho}_i) dm_i \tag{5.13}$$

Introducing Eqs. (5.4) - (5.6) into Eq. (5.13), we obtain

$$\tilde{\phi}_i^T = \rho \int_{(4-i)h}^{(5-i)h} [L_1(46 + z^*)\ hL_2(46 + z^*)\ L_3(46 + z^*)\ hL_4(46 + z^*)]^T dz^* \tag{5.14}$$

Carrying out the above integration, we have

$$\tilde{\phi}_i^T = \rho[23h + h^2(43/20 - i/2) \quad (121/130)h^2 + (2-i)h^3/12$$

$$23h + (43/20 - i/2)h^2 \quad - 23h^2/6 + (10i - 46)h^3/120]^T \qquad (5.15)$$

Finally, Φ, $\bar{\Phi}$ and $\tilde{\Phi}^T$ are obtained by assembling ϕ_i, $\bar{\phi}_i$ and $\tilde{\phi}^T$, respectively. The results are

$$\Phi = \left[\frac{1}{2}\rho h \quad \frac{1}{12}\rho h^2 \quad \rho h \quad 0 \quad \rho h \quad 0 \quad \rho h \quad 0\right] \qquad (5.16a)$$

$$
\underline{\Phi} = \begin{bmatrix}
\frac{13}{325}\rho h & & & & & & & \\
\frac{11}{210}\rho h^2 & \frac{1}{105}\rho h^3 & & & & & & \\
\frac{9}{70}\rho h & \frac{13}{420}\rho h^2 & \frac{34}{35}\rho h & & & \text{Symm} & & \\
\frac{-13}{420}\rho h^2 & \frac{-1}{420}\rho h^2 & 0 & \frac{2}{105}\rho h^3 & & & & \\
0 & 0 & \frac{9}{70}\rho h & \frac{13}{420}\rho h^2 & \frac{34}{35}\rho h & & & \\
0 & 0 & \frac{-13}{420}\rho h^2 & \frac{-1}{420}\rho h^2 & 0 & \frac{2}{105}\rho h^3 & & \\
0 & 0 & 0 & 0 & \frac{9}{70}\rho h & \frac{13}{420}\rho h^2 & \frac{34}{35}\rho h & \\
0 & 0 & 0 & 0 & \frac{-13}{420}\rho h^2 & \frac{-1}{140}\rho h^2 & 0 & \frac{2}{105}\rho h^2
\end{bmatrix}
$$

(5.16b)

$$\tilde{\Phi} = \begin{bmatrix} h(23 + \frac{33h}{20}) \\ h^2(\frac{121}{130} + \frac{h}{12}) \\ h(46 + 3h) \\ h^2(\frac{-3h}{10} - \frac{23}{6} + \frac{121}{130}) \\ h(46 + 2h) \\ h^2(\frac{-3h}{10} - \frac{23}{6} + \frac{121}{130}) \\ h(46 + h) \\ h^2(\frac{-3h}{10} - \frac{23}{6} + \frac{121}{130}) \end{bmatrix} \qquad (5.16c)$$

The element stiffness matrix K_i corresponding to the displacements in the x direction is

$$K_i = \begin{bmatrix} \frac{12EI_{yy}}{l^3} & & & \\ \frac{6EI_{yy}}{l^2} & \frac{4EI_{yy}}{l} & \text{Symm} & \\ \frac{-12EI_{yy}}{l^3} & \frac{-6EI_{yy}}{l^2} & \frac{12EI_{yy}}{l^3} & \\ \frac{6EI_{yy}}{l^2} & \frac{2EI_{yy}}{l} & \frac{-6EI_{yy}}{l^2} & \frac{4EI_{yy}}{l} \end{bmatrix} \qquad (5.17)$$

So that, assembling K_i, we obtain

$$K_F = \begin{bmatrix}
\frac{12EI_{yy}}{l^3} & & & & & & & \\
\frac{6EI_{yy}}{l^2} & \frac{4EI_{yy}}{l} & & & & & & \\
\frac{-12EI_{yy}}{l^3} & \frac{-6EI_{yy}}{l^2} & \frac{24EI_{yy}}{l^3} & & & \text{Symm} & & \\
\frac{6EI_{yy}}{l^2} & \frac{2EI_{yy}}{l} & 0 & \frac{8EI_{yy}}{l} & & & & \\
0 & 0 & \frac{-12EI_{yy}}{l^3} & \frac{-6EI_{yy}}{l^2} & \frac{24EI_{yy}}{l} & & & \\
0 & 0 & \frac{6EI_{yy}}{l^2} & \frac{2EI_{yy}}{l} & 0 & \frac{8EI_{yy}}{l} & & \\
0 & 0 & 0 & 0 & \frac{-12EI_{yy}}{l^3} & \frac{-6EI_{yy}}{l^2} & \frac{24EI_{yy}}{l^3} & \\
0 & 0 & 0 & 0 & \frac{6EI_{yy}}{l^2} & \frac{2EI_{yy}}{l} & 0 & \frac{8EI_{yy}}{l}
\end{bmatrix} \tag{5.18}$$

5.3 RESULTS AND DISCUSSIONS

The open-loop eigenvalues are displayed in Table 5.2 and the submatrices P_{11} and P_{31}, P_{21}, P_{41}, P_{22}, P_{42} are displayed in Tables 5.3 - 5.8. The first four eigenvalues correspond to the modes associated with the motion of the rigid platform and the remaining to the modes associated with the motion of the flexible structure. It can be seen that the modes of the flexible structure have essentially no damping. Submatrices P_{12} and P_{32} are essentially null matrices, confirming expectations. An examination of the submatrices P_{22} and P_{42} shows that the columns occur as interdependent pairs, in accordance with the analysis presented in Ref. 6. Finally, an examination of the submatrices P_{11} and P_{31} shows that the rigid-body modes correspond to the longitudinal motion x and the remaining mode corresponds to the pitching motion ψ, indicating that the two motions x and ψ have negligible influence on each other. This enables us to control each mode independently. We choose to control the modes associated with the rigid platform and the first four modes associated with the flexible structure. The control gain matrix G_c is shown in Table 5.9. The closed-loop eigenvalues are displayed in Table 5.2. In the design of the observer, only the velocities were measured and used for feedback. The observer eigenvalues are also shown in Table 5.2. The observer gain matrix is shown in Table 5.10. The uncontrolled and controlled responses of the longitudinal motion and the pitching motion of the platform, and the nodes of the cantilever beam are shown in Figs. 5.10 - 5.21. The time history of the control forces are shown in Figs. 5.22 - 5.27. Examination of the responses shows that the controlled responses

are about 50% smaller in magnitude than the corresponding uncontrolled responses. Examination of the responses also show that the time history of the estimated velocities of the controlled flexible structure exhibit noise envelopes within which the velocities are confined. The envelopes can be attributed to the random nature of the measured velocities. Inspection of the control force time histories shows that the estimated control forces for a segment of a spectrum are free of the noise envelopes observed in the estimated velocity responses. The differences between the RMS values of the measured velocities and estimated velocities after 120 seconds of simulation were around 10% of the corresponding measured velocities.

Table 5.1 Dimensions of the Structure

Diameter of upper cylinder	$D_1 = 32$ m
Diameter of lower cylinder	$D_2 = 52$ m
Underwater height of upper cylinder	$H_1 = 15$ m
Height of lower cylinder	$H_2 = 44$ m
Depth of water	$H_3 = 100$ m
Volume of water displaced	$V = 105500\ m^3$
Mass of structure	$M = 1.1 \times 10^8$ kg
Center of gravity above base	GK = 23 m
Center of buoyancy above base	FK = 25.37 m
Radius of gyration around x, y axes	$i_{xx} = i_{yy} = 19.75$ m
Moment of inertia around x, y axes	$M_\phi = M_\psi = 4.3 \times 10^{10}\ kg \cdot m^2$
Radius of gyration around z-axis	$i_{zz} = 15.6$ m
Moment of inertia around z-axis	$M_\nu = 2.6 \times 10^{10}\ kg \cdot m^2$
Height of cantilever	$H_4 = 10$ m
Length of cantilever	$L_y = 0.1$ m
Width of cantilever	$L_x = 0.05$ m
Mass per meter of cantilever	$\rho = 39.3$ kg/m

Table 5.2 Eigenvalues

Open loop poles	Closed loop poles	Observer Poles
0.0	0.0	0.0
-0.0270	-0.0400	-0.0274
-0.0005 ± i 0.2120	-0.0850 ± i 0.2133	-0.0162 ± i 0.0624
0.0 ± i 2.4084	-0.2234 ± i 2.4804	-0.3356 ± i 2.8894
0.0 ± i 14.8747	-0.0707 ± i 14.8750	-1.5806 ± i 12.8703
0.0 ± i 41.3667	-0.0707 ± i 41.3070	-0.5981 ± i 40.8849
0.0 ± i 77.7629	0.0 ± i 77.7629	0.0 ± i 77.7628
0.0 ± i 192.3846	0.0 ± i 192.3846	0.0 ± i 192.3846
0.0 ± i 285.3756	0.0 ± i 285.3756	0.0 ± i 285.3756
0.0 ± i 341.9900	0.0 ± i 341.9900	0.0 ± i 341.9900
0.0 ± i 448.5287	0.0 ± i 448.5287	0.0 ± i 448.5287

Table 5.3 Submatrix P_{11}

0.00000D 00	0.39056D 00	-0.86464D-03	-0.15656D-01
0.00000D 00	-0.10637D-04	0.14799D-02	0.13259D-01

Table 5.4 Submatrix P_{31}

0.14142D 01	-0.14186D 02	-0.73849D-01	0.42429D-02
0.00000D 00	0.38634D-03	0.62535D-01	-0.71203D-02

Table 5.5 Submatrix P_{21}

0.00000D 00	-0.69715D-04	0.67372D-03	0.62031D-02
0.00000D 00	0.92954D-05	-0.88562D-04	-0.81526D-03
0.00000D 00	-0.46567D-04	0.45299D-03	0.41712D-02
0.00000D 00	0.91501D-05	-0.87681D-04	-0.80722D-03
0.00000D 00	-0.24690D-04	0.24204D-03	0.22290D-02
0.00000D 00	0.81333D-05	-0.79066D-04	-0.72804D-03
0.00000D 00	-0.73526D-05	0.72547D-04	0.66815D-03
0.00000D 00	0.53738D-05	-0.52933D-04	-0.48749D-03

Table 5.6 Submatrix P_{41}

0.00000D 00	0.25322D-02	0.29257D-01	-0.32432D-02
0.00000D 00	-0.33763D-03	-0.38452D-02	0.42633D-03
0.00000D 00	0.16914D-02	0.19673D-01	-0.21807D-02
0.00000D 00	-0.33235D-03	-0.38072D-02	0.42209D-03
0.00000D 00	0.89679D-03	0.10513D-01	-0.11652D-02
0.00000D 00	-0.29542D-03	-0.34338D-02	0.38062D-03
0.00000D 00	0.26706D-03	0.31513D-02	-0.34924D-03
0.00000D 00	-0.19518D-03	-0.22993D-02	0.25482D-03

Table 5.7 Submatrix P_{22}

-0.86850D 00	0.17601D 01	-0.39950D 01	-0.60165D 01
0.11886D 00	-0.24089D 00	0.18109D 01	0.27272D 01
-0.57281D 00	0.11608D 01	0.30918D 00	0.46562D 00
0.11658D 00	-0.23626D 00	0.14888D 01	0.22421D 01
-0.29664D 00	0.60117D 00	0.25841D 01	0.38917D 01
0.10124D 00	-0.20516D 00	0.21384D 00	0.32204D 00
-0.85250D-01	0.17277D 00	0.15518D 01	0.23370D 01
0.63708D-01	-0.12911D 00	-0.83860D 00	-0.12629D 01

0.70438D 01	0.31843D 01	-0.10733D 02	0.10003D 02	0.17256D 01	-0.34328D 02	0.11259D 02	-0.38365D 02
-0.51937D 01	-0.23479D 01	0.10787D 02	-0.10053D 02	-0.23979D 01	0.47702D 02	-0.14258D 02	0.48582D 02
-0.34618D 01	-0.15650D 01	0.63905D 01	-0.59559D 01	-0.48478D 00	0.96436D 01	-0.30092D 00	0.10253D 01
-0.18377D 01	-0.83079D 00	-0.18652D 01	0.17383D 01	0.22604D 01	-0.44966D 02	0.23458D 02	-0.79930D 02
0.85340D-02	0.38806D-02	-0.75573D 01	0.70433D 01	0.11173D 00	-0.22227D 01	-0.56766D 01	0.19342D 02
0.33655D 01	0.15214D 01	-0.10985D 00	0.10238D 00	-0.32379D 01	0.64411D 02	-0.88939D 01	0.30305D 02
0.45856D 01	0.20730D 01	0.70517D 01	-0.65722D 01	0.46336D 00	-0.92176D 01	0.18830D 01	-0.64160D 01
-0.88587D 00	-0.40048D 00	0.31520D 01	-0.29376D 01	0.29782D 01	-0.59244D 02	-0.25893D 02	0.88228D 02

0.26029D 02	-0.71819D 01	-0.44899D 01	-0.77826D 02
0.25420D 02	-0.70137D 01	0.13670D 02	0.23695D 03
0.93457D 01	-0.25786D 01	-0.74250D 00	-0.12870D 02
0.14268D 03	-0.39367D 02	-0.92598D 00	-0.16051D 02
-0.69047D 01	0.19051D 01	0.15976D 00	0.27691D 01
0.14721D 03	-0.40617D 02	-0.11994D 01	-0.20790D 02
-0.13745D 02	0.37925D 01	0.87004D-01	0.15081D 01
0.67330D 02	-0.18577D 02	-0.20571D 00	-0.35658D 01

Table 5.8 Submatrix P_{42}

0.73081D 00	0.36061D 00	-0.40448D 00	0.26858D 00
-0.10002D 00	-0.49354D-01	0.18334D 00	-0.12174D 00
0.48200D 00	0.23784D 00	0.31303D-01	-0.20785D-01
-0.98097D-01	-0.48405D-01	0.15073D 00	-0.10009D 00
0.24961D 00	0.12317D 00	0.26163D 00	-0.17373D 00
-0.85186D-01	-0.42034D-01	0.21650D-01	-0.14376D-01
0.71735D-01	0.35397D-01	0.15712D 00	-0.10433D 00
-0.53608D-01	-0.26452D-01	-0.84905D-01	0.56377D-01

0.76978D-01	-0.17028D 00	0.12864D 00	0.13803D 00	-0.17843D 00	-0.89697D-02	-0.13444D 00	-0.39455D-01
-0.56759D-01	0.12555D 00	-0.12928D 00	-0.13871D 00	0.24795D 00	0.12464D-01	0.17024D 00	0.49962D-01
-0.37832D-01	0.83686D-01	-0.76590D-01	-0.82179D-01	0.50127D-01	0.25198D-02	0.35929D-02	0.10545D-02
-0.20084D-01	0.44426D-01	0.22354D-01	0.23985D-01	-0.23373D 00	-0.11749D-01	-0.28009D 00	-0.82200D-01
0.93809D-04	-0.20751D-03	0.90574D-01	0.97183D-01	-0.11553D-01	-0.58077D-03	0.67778D-01	0.19892D-01
0.36779D-01	-0.81357D-01	0.13165D-02	0.14126D-02	0.33481D 00	0.16830D-01	0.10619D 00	0.31165D-01
0.50114D-01	-0.11085D 00	-0.84516D-01	-0.90683D-01	-0.47912D-01	-0.24085D-02	-0.22483D-01	-0.65982D-02
-0.96811D-02	0.21415D-01	-0.37777D-01	-0.40533D-01	-0.30795D 00	-0.15480D-01	0.30916D 00	0.90734D-01

-0.21000D-01	-0.76111D-01	-0.17352D 00	0.10010D-01
-0.20508D-01	-0.74329D-01	0.52828D 00	-0.30477D-01
-0.75401D-02	-0.27327D-01	-0.28694D-01	0.16554D-02
-0.11511D 00	-0.41720D 00	-0.35785D-01	0.20645D-02
0.55707D-02	0.20190D-01	0.61738D-02	-0.35618D-03
-0.11877D 00	-0.43045D 00	-0.46351D-01	0.26740D-02
0.11089D-01	0.40191D-01	0.33623D-02	-0.19398D-03
-0.54321D-01	-0.19688D 00	-0.79499D-02	0.45864D-03

Table 5.9 Feedback Gain-Matrix G_c

0	0	0	0	0	0	0	0	0	0
0	-0.0665	0	0	0	0	0	0	0	0
0	0	0	0	0	0	0	0	0	0
0	0	-0.0325	-0.1691	0	0	0	0	0	0
0	0	0	0	0	0	0	0	0	0
0	0	0	0	-0.0207	-0.4467	0	0	0	0
0	0	0	0	0	0	0	0	0	0
0	0	0	0	0	0	-0.0034	-0.1414	0	0
0	0	0	0	0	0	0	0	0	0
0	0	0	0	0	0	0	0	-0.0012	-0.1421

Table 5.10 Observer-Gain Matrix μ

$$\begin{bmatrix} 0.1 & & & & & & & \\ & 0.1 & & & & & & \\ & & -0.1 & & & & & \\ & & & -0.1 & & & & \\ & & & & -1.0 & & & \\ & & & & & -1.0 & & \\ & & & & & & 1.0 & \\ & & & & & & & 1.0 \\ & & & & & & & \\ & & & & & & & \end{bmatrix}$$

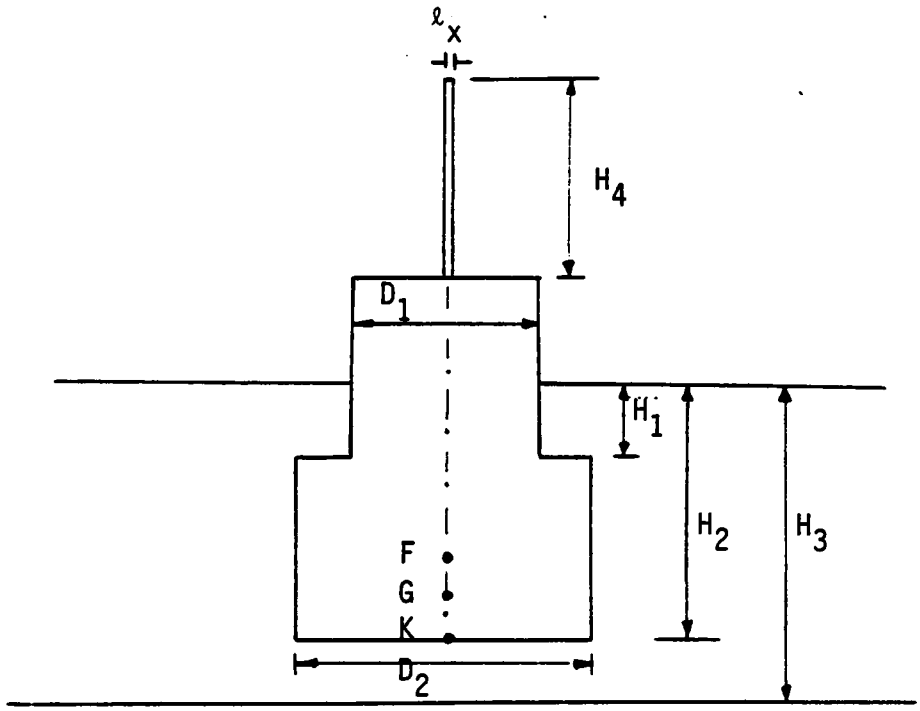

Fig. 5.1 - The Mathematical Model

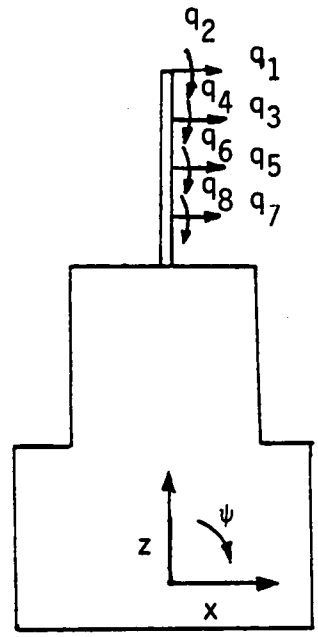

Fig. 5.2 - System of Coordinates

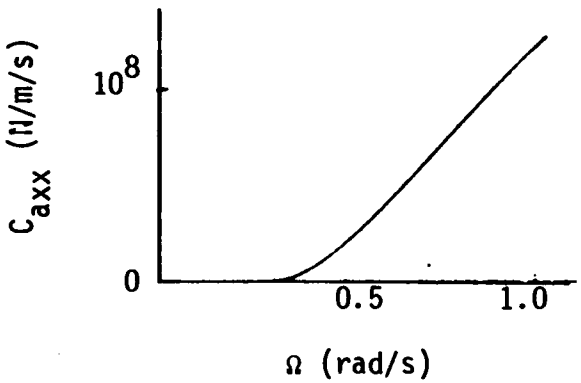

Fig. 5.3 Longitudinal Potential Damping

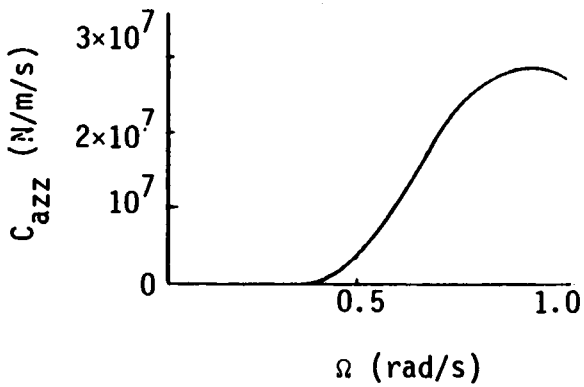

Fig. 5.4 Vertical Potential Damping

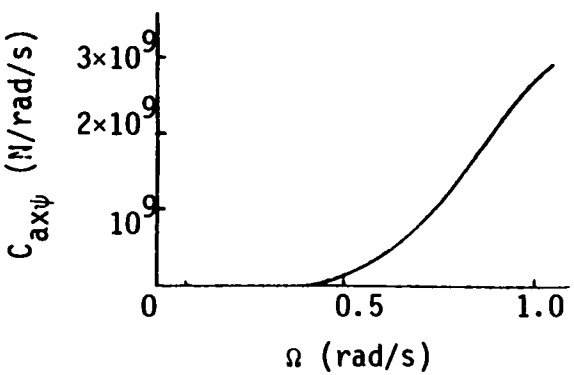

Fig. 5.5 Coupled Potential Damping Between Surge and Pitch

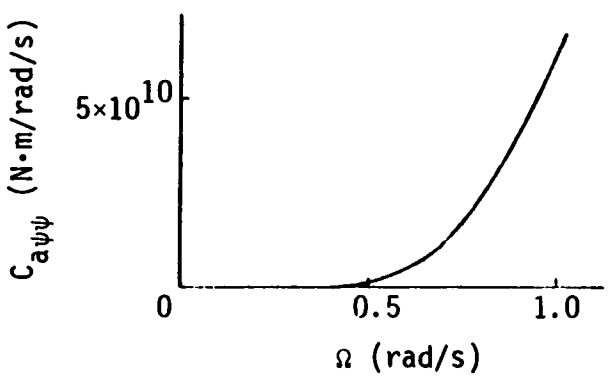

Fig. 5.6 Pitch Potential Damping

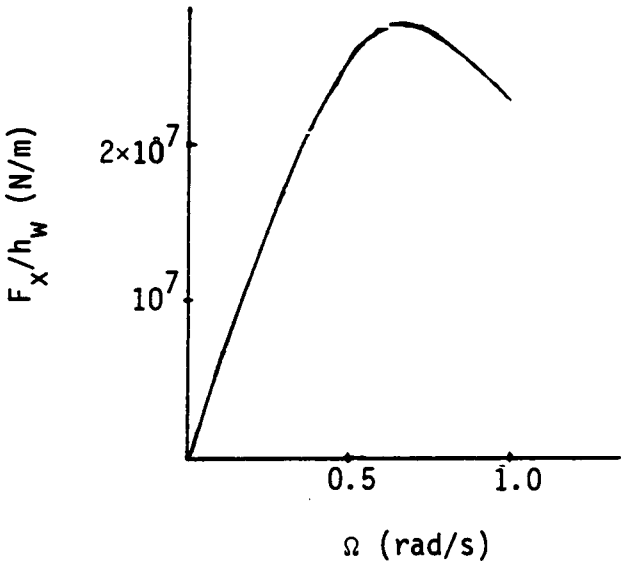

Fig. 5.7 Longitudinal Wave Excited Force

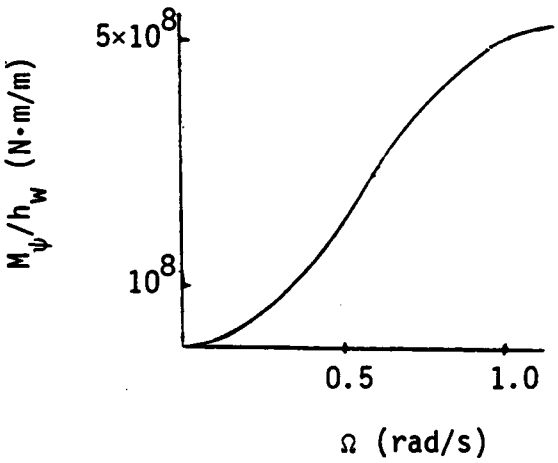

Fig. 5.8 Wave-Excited Pitching Moment

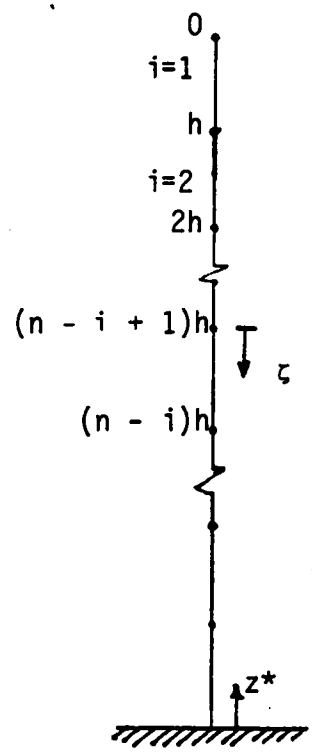

Fig. 5.9 Local and Global Coordinate System of the Cantilever Beam

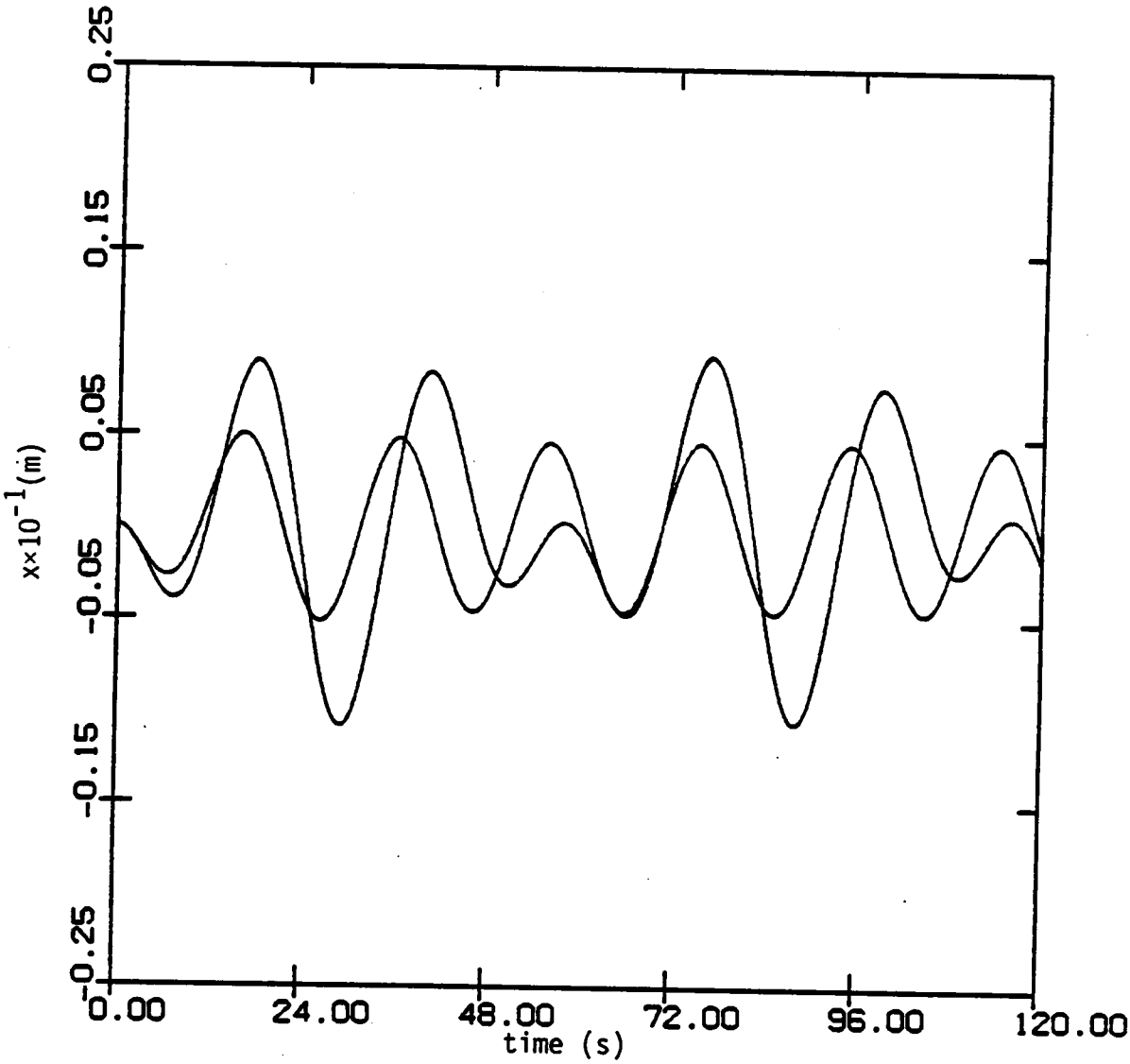

Fig. 5.10 Longitudinal Displacement x vs Time

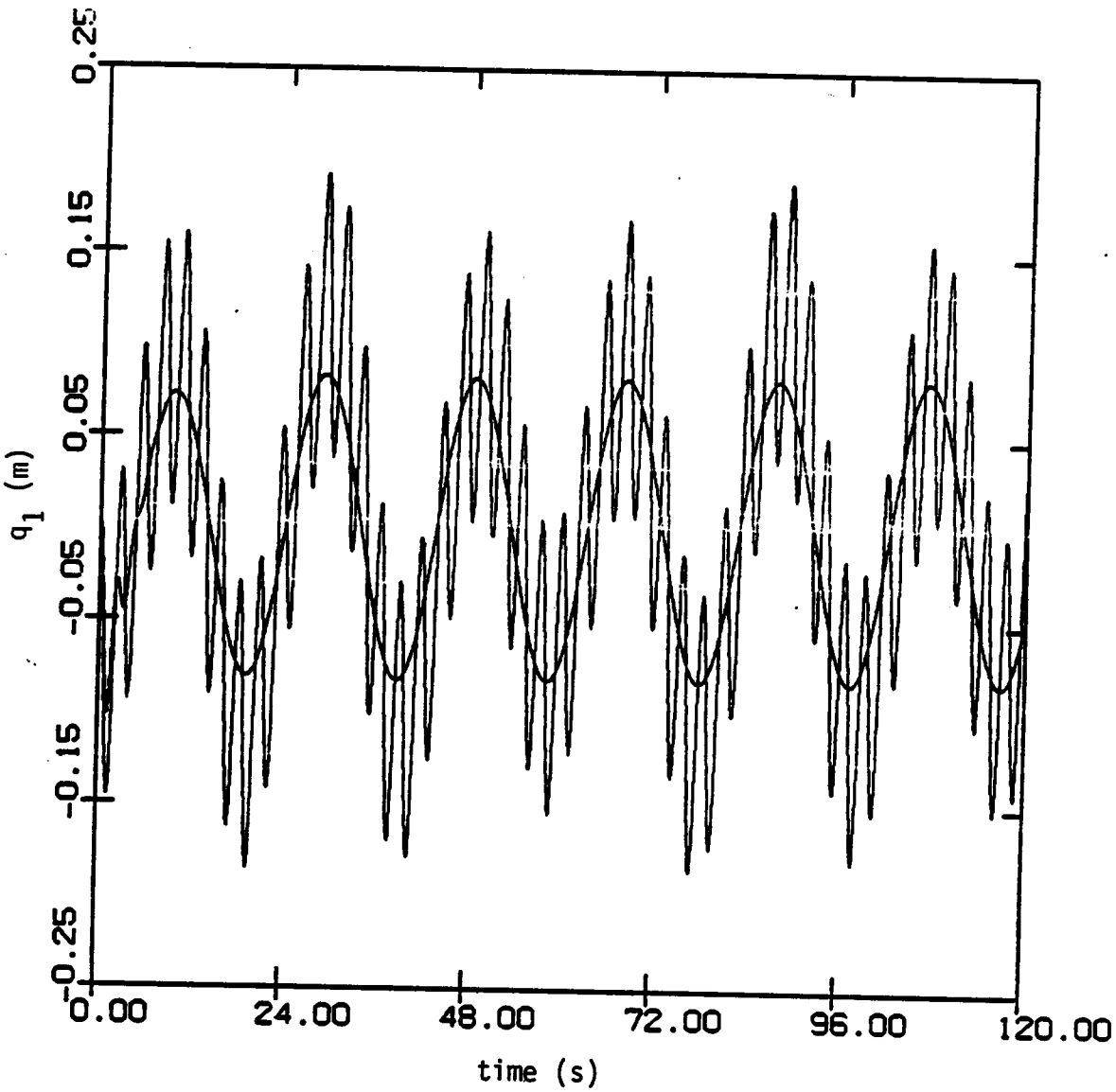

Fig. 5.11 Longitudinal Displacement q_1 vs Time

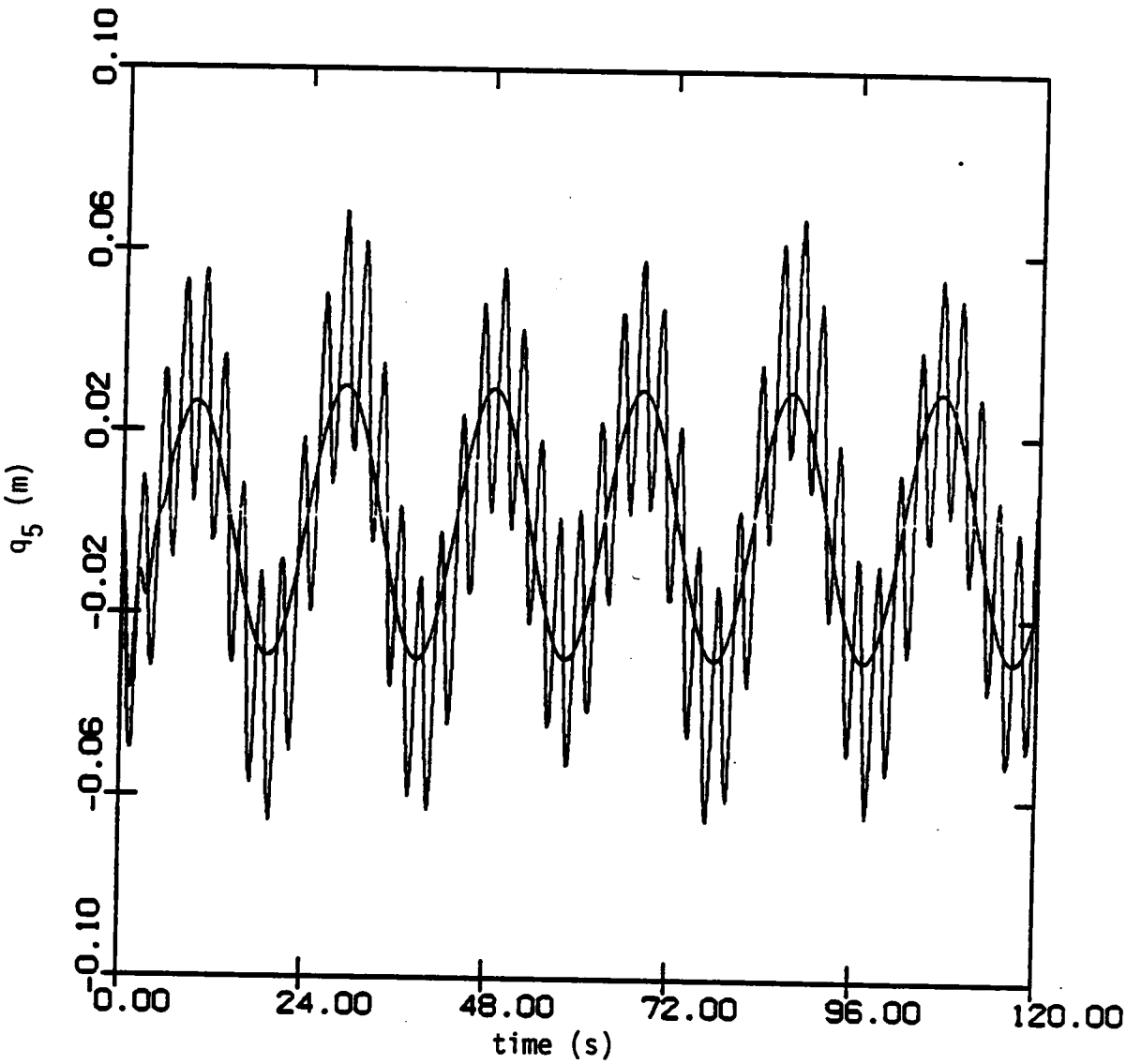

Fig. 5.12 Longitudinal Displacemnt q_5 vs Time

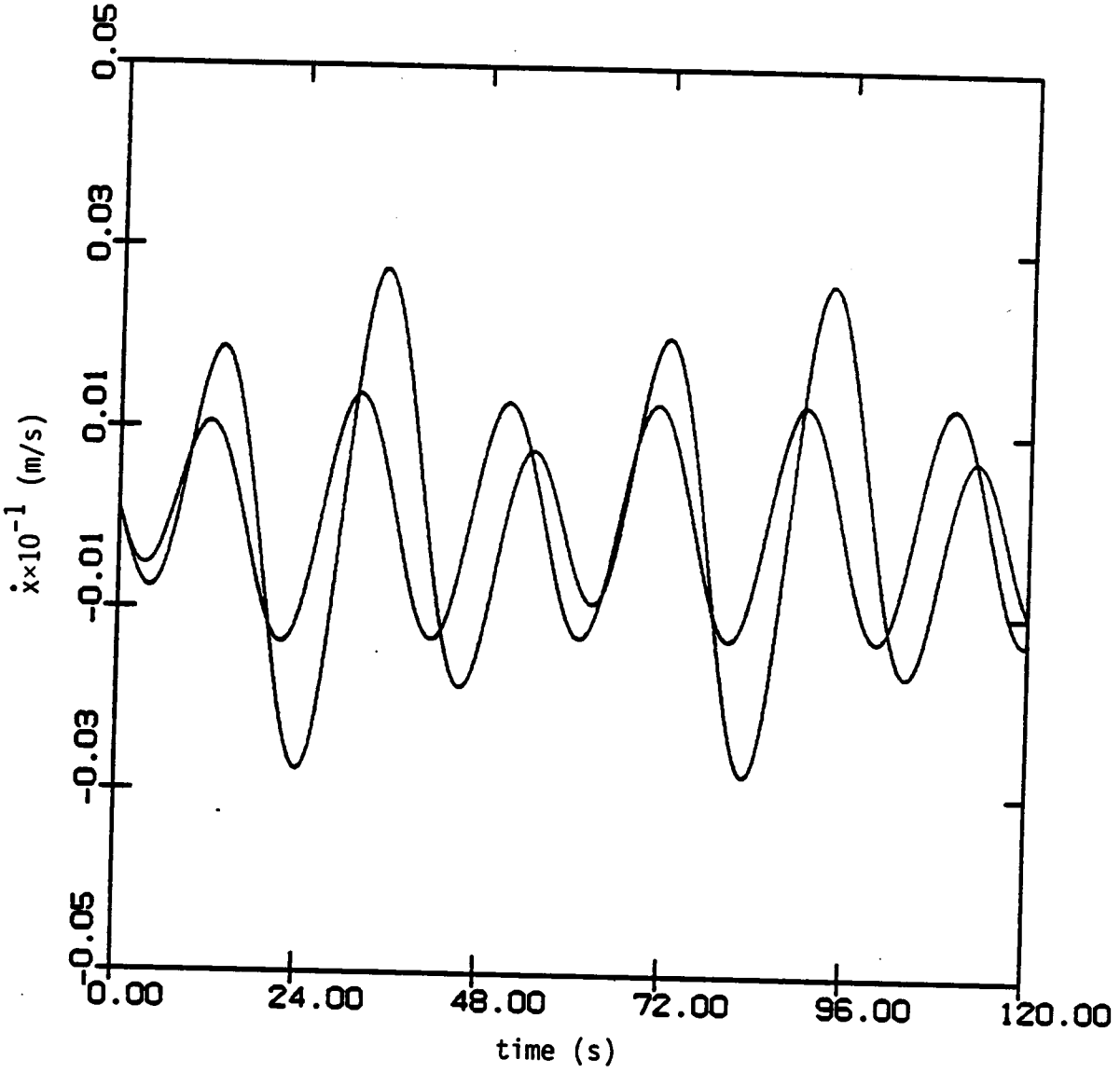

Fig. 5.13 Longitudinal Velocity $\dot{x}$ vs Time

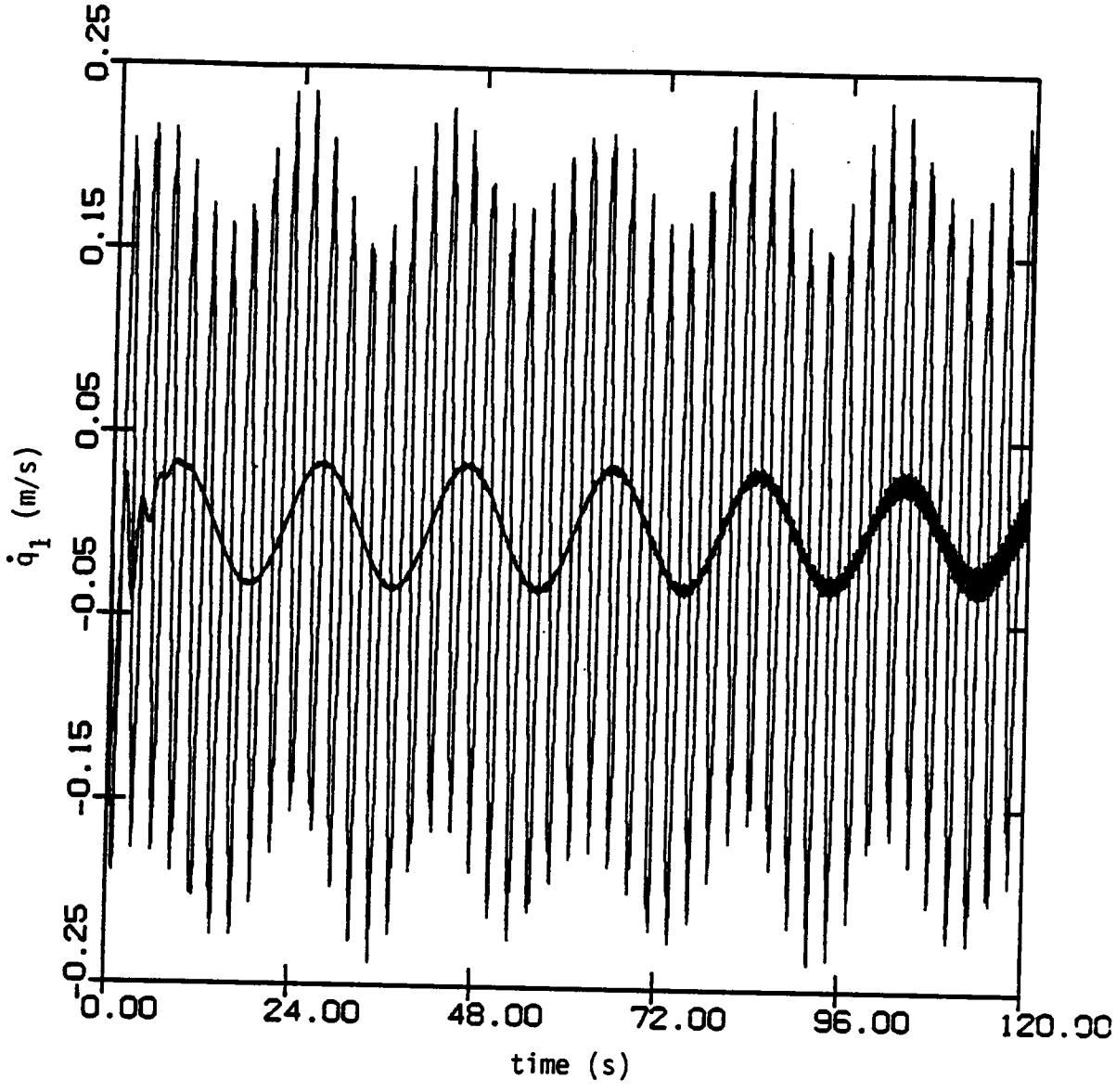

Fig. 5.14 Longitudinal Velocity $\dot{q}_1$ vs Time

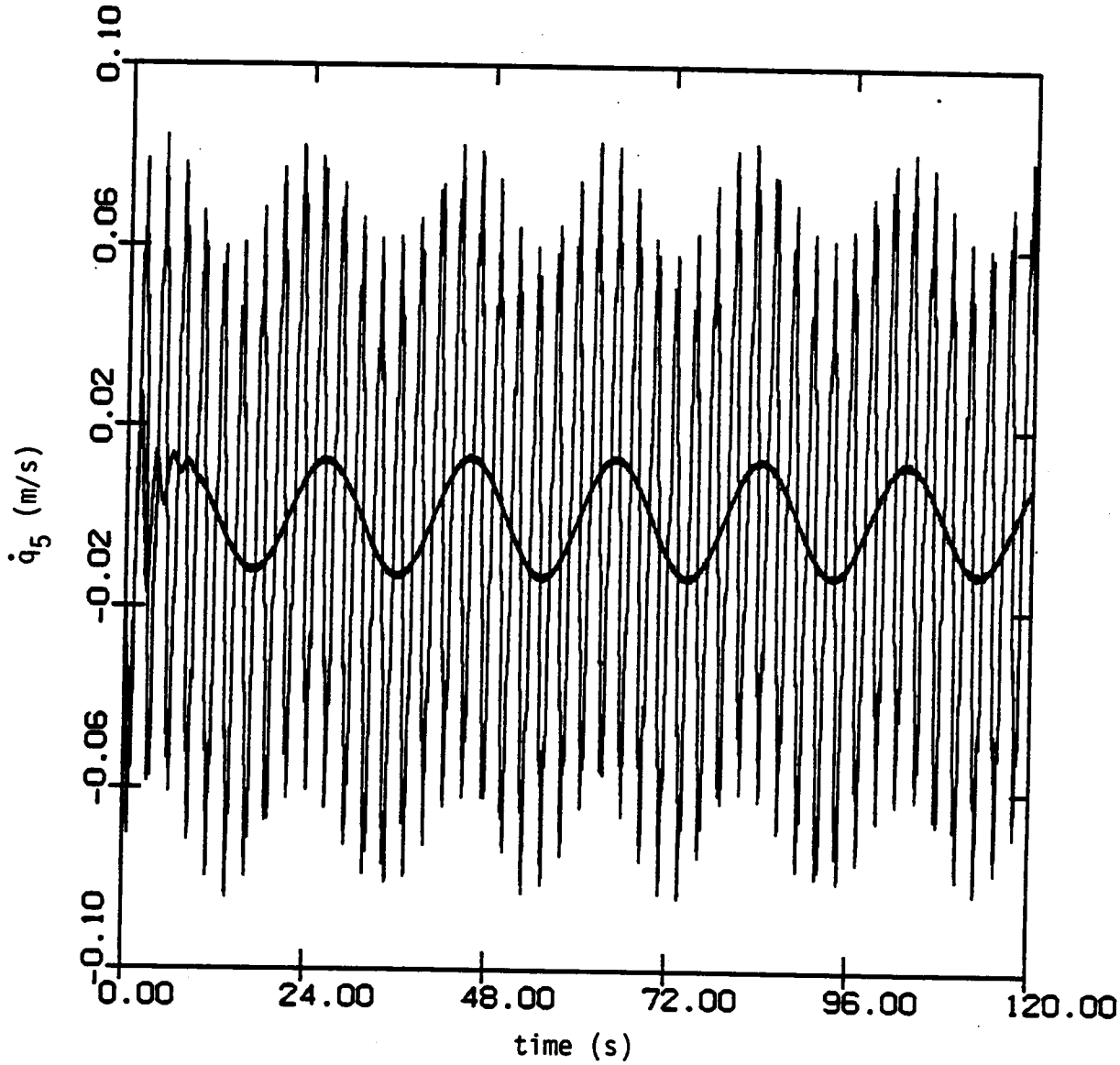

Fig. 5.15 Longitudinal Velocity $\dot{q}_5$ vs Time

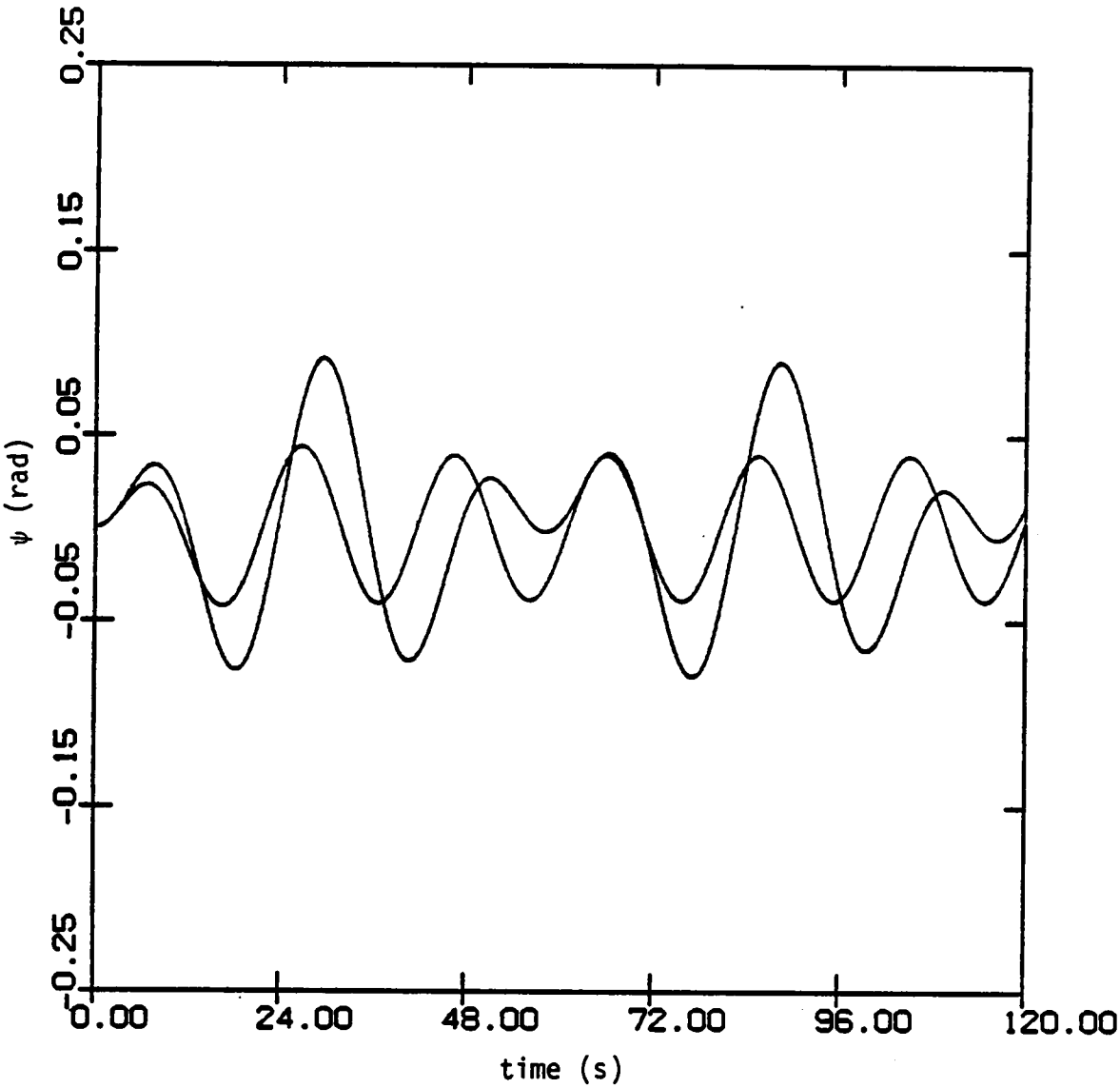

Fig. 5.16 Angular Displacement ψ vs Time

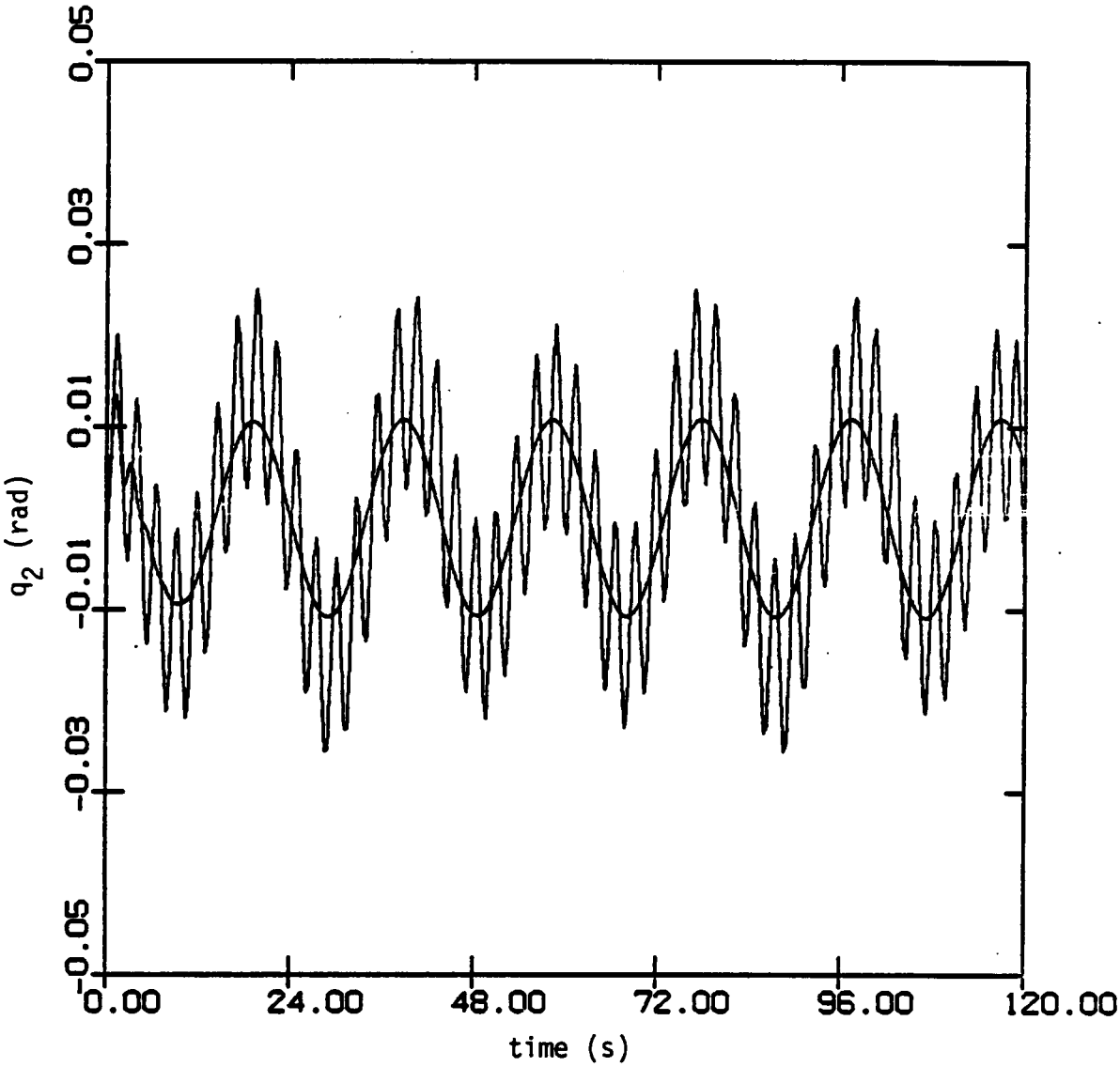

Fig. 5.17 Angular Displacement q_2 vs Time

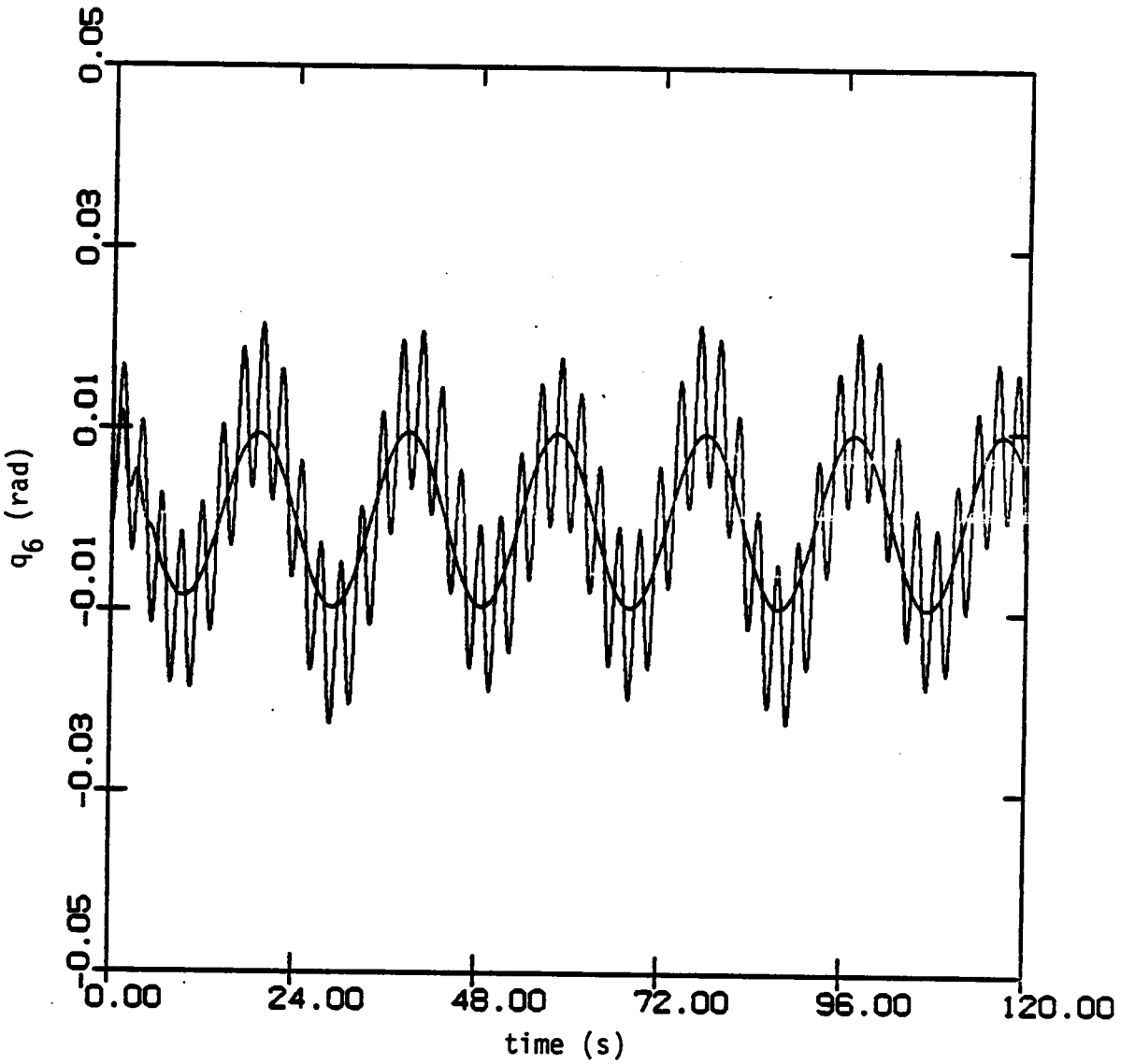

Fig. 5.18 Angular Displacement q_6 vs Time

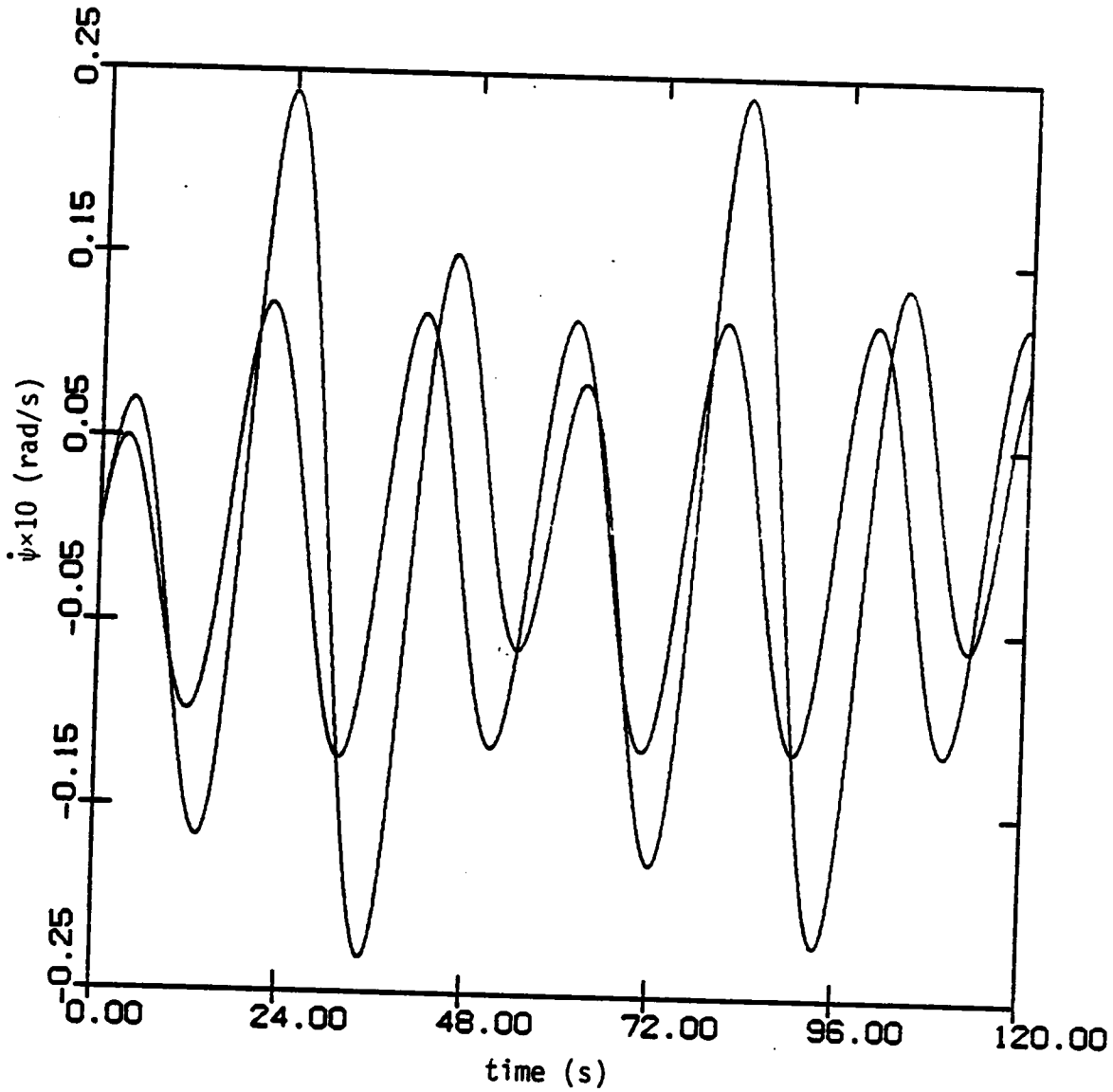

Fig. 5.19 Angular Velocity $\dot{\psi}$ vs Time

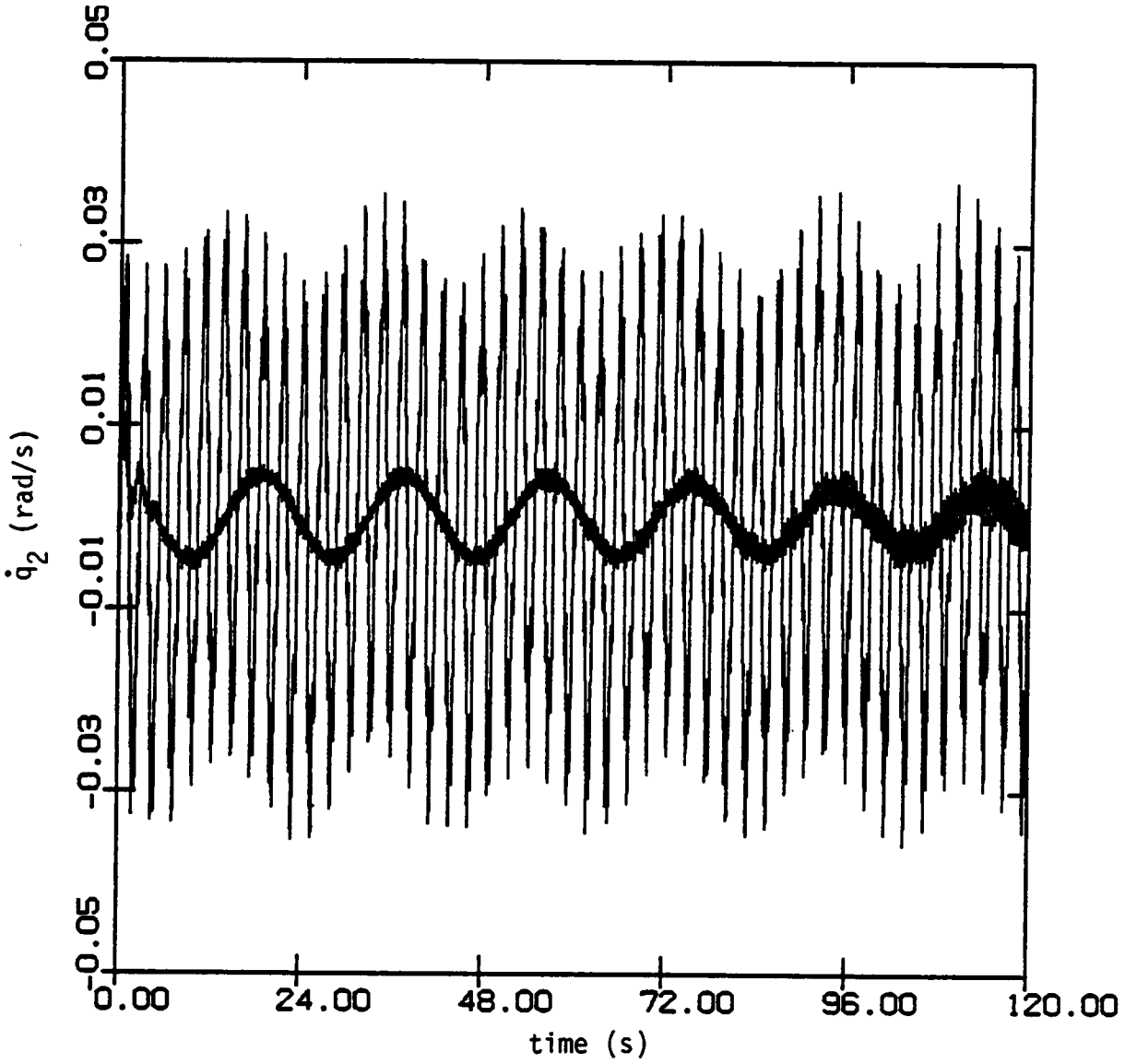

Fig. 5.20 Angular Velocity $\dot{q}_2$ vs Time

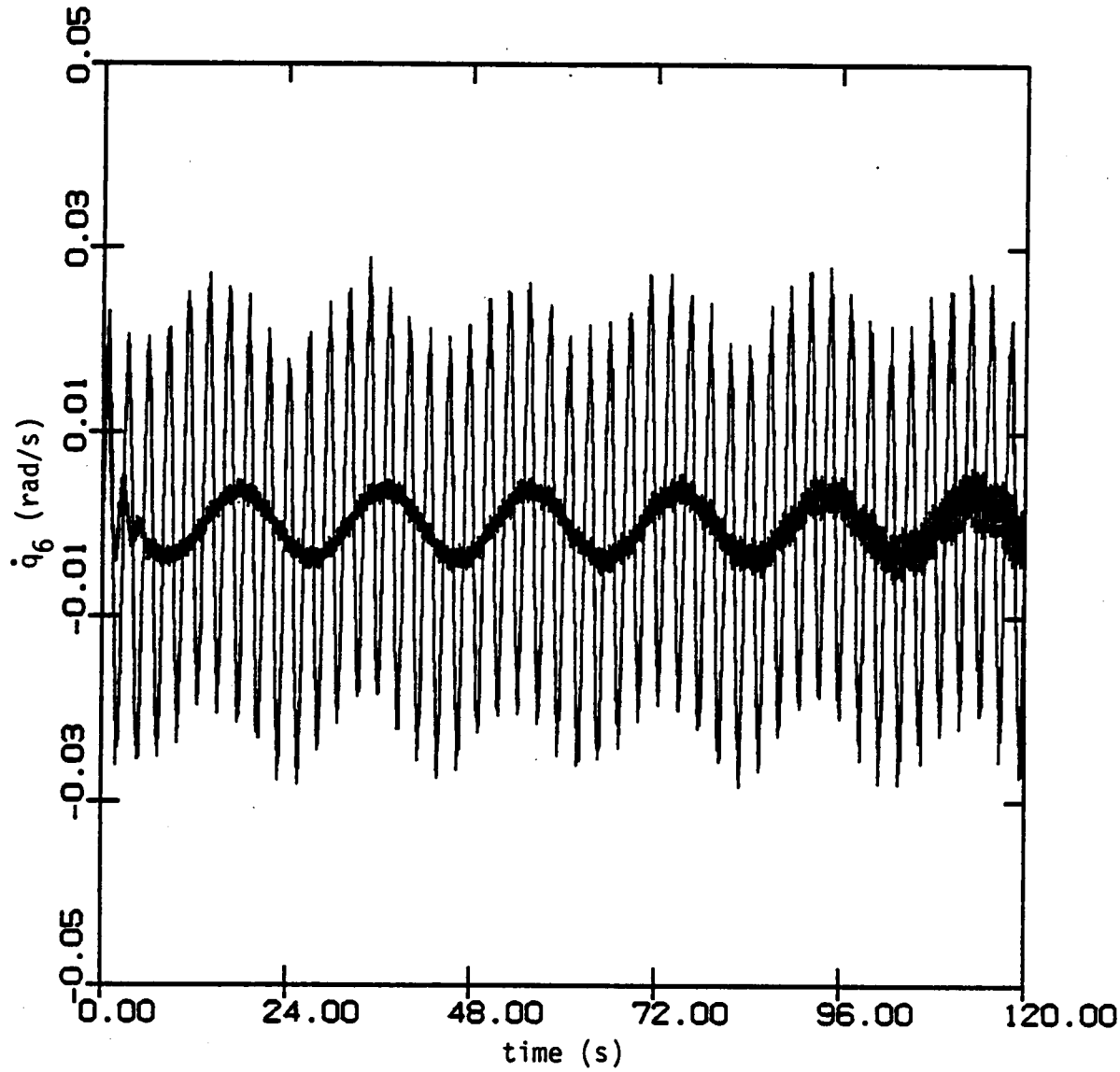

Fig. 5.21 Angular Velocity $\dot{q}_6$ vs Time

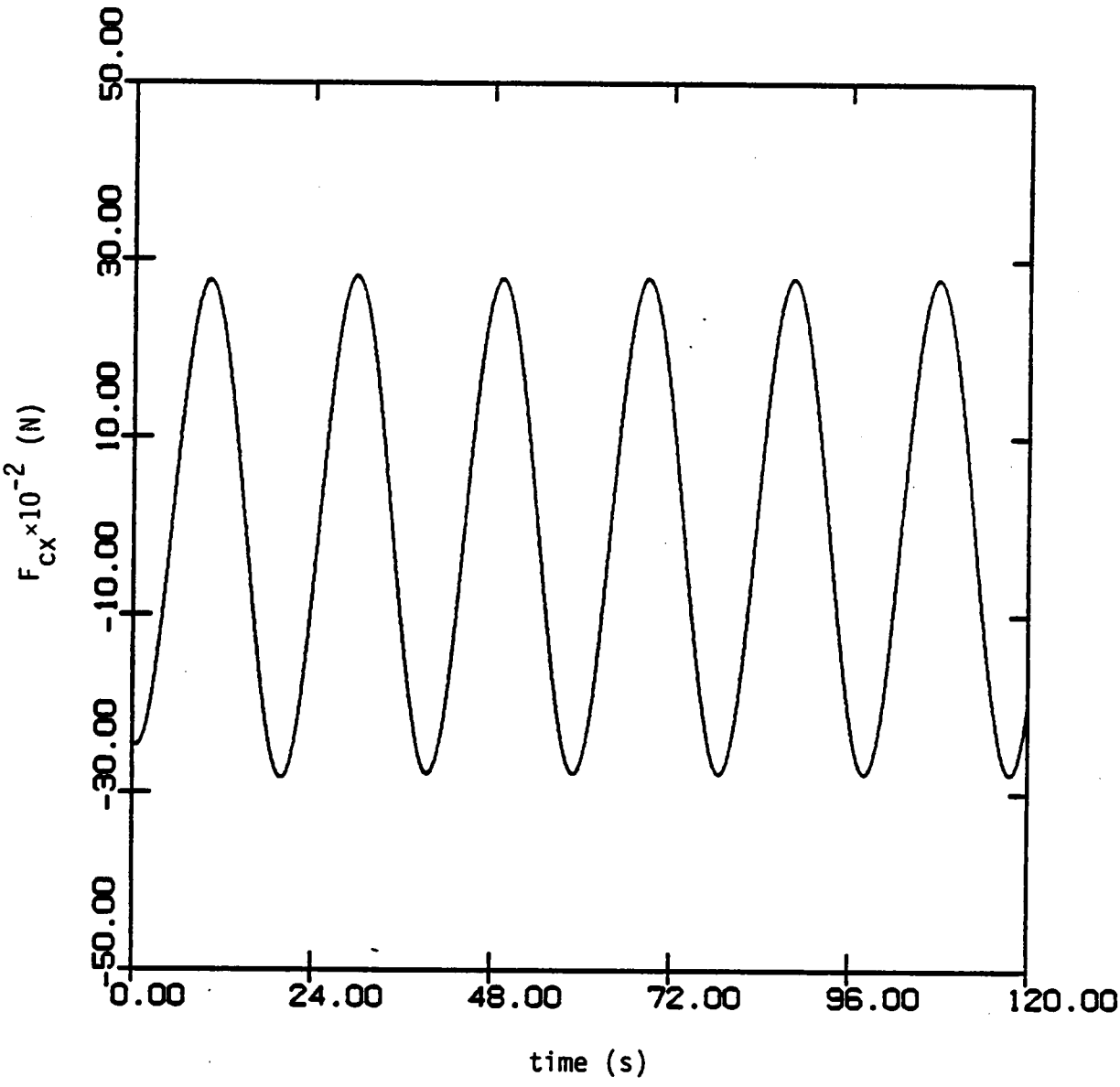

Fig. 5.22 Control Force F_{cx} vs Time

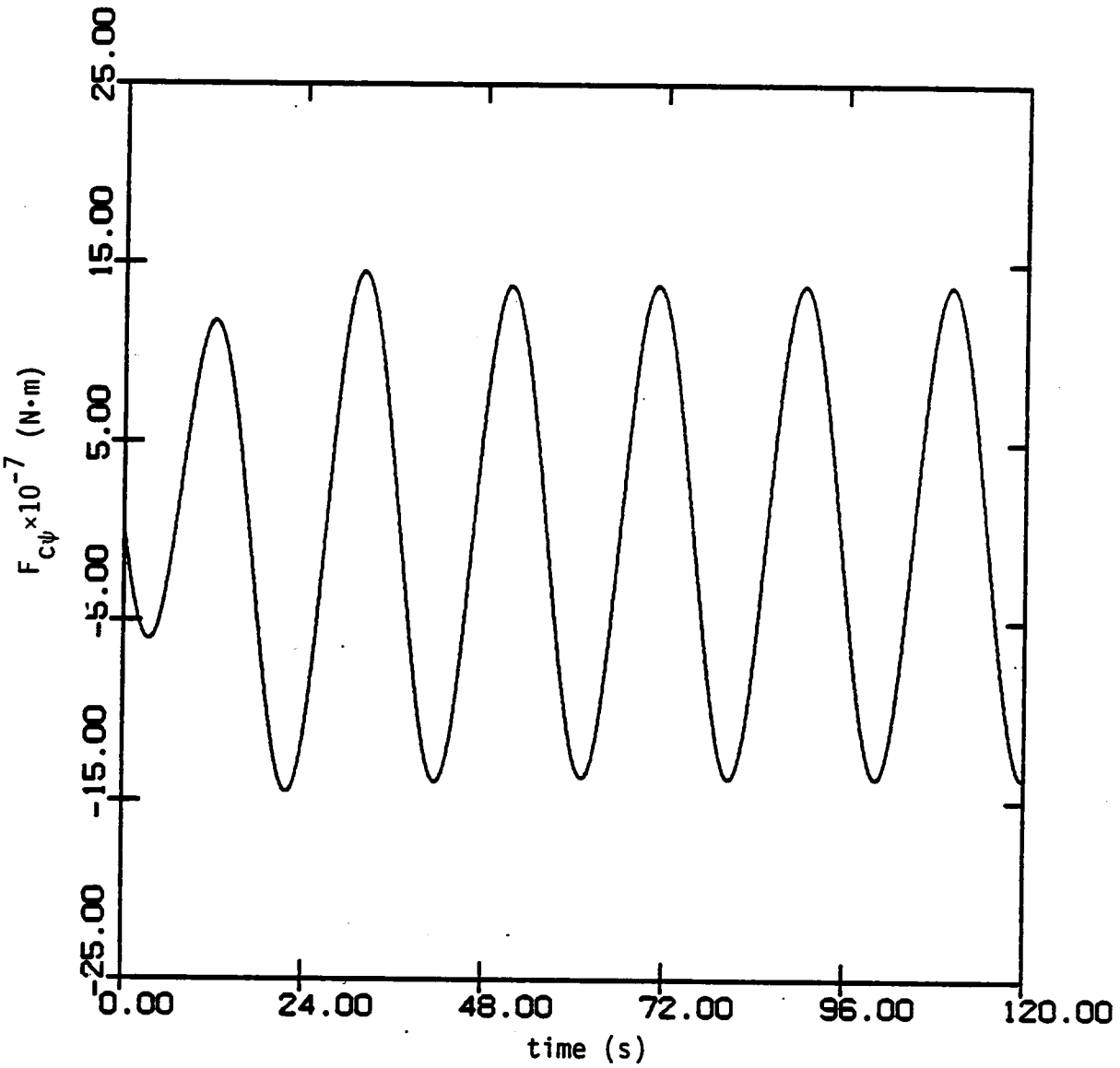

Fig. 5.23 Control Torque $F_{C\psi}$ vs Time

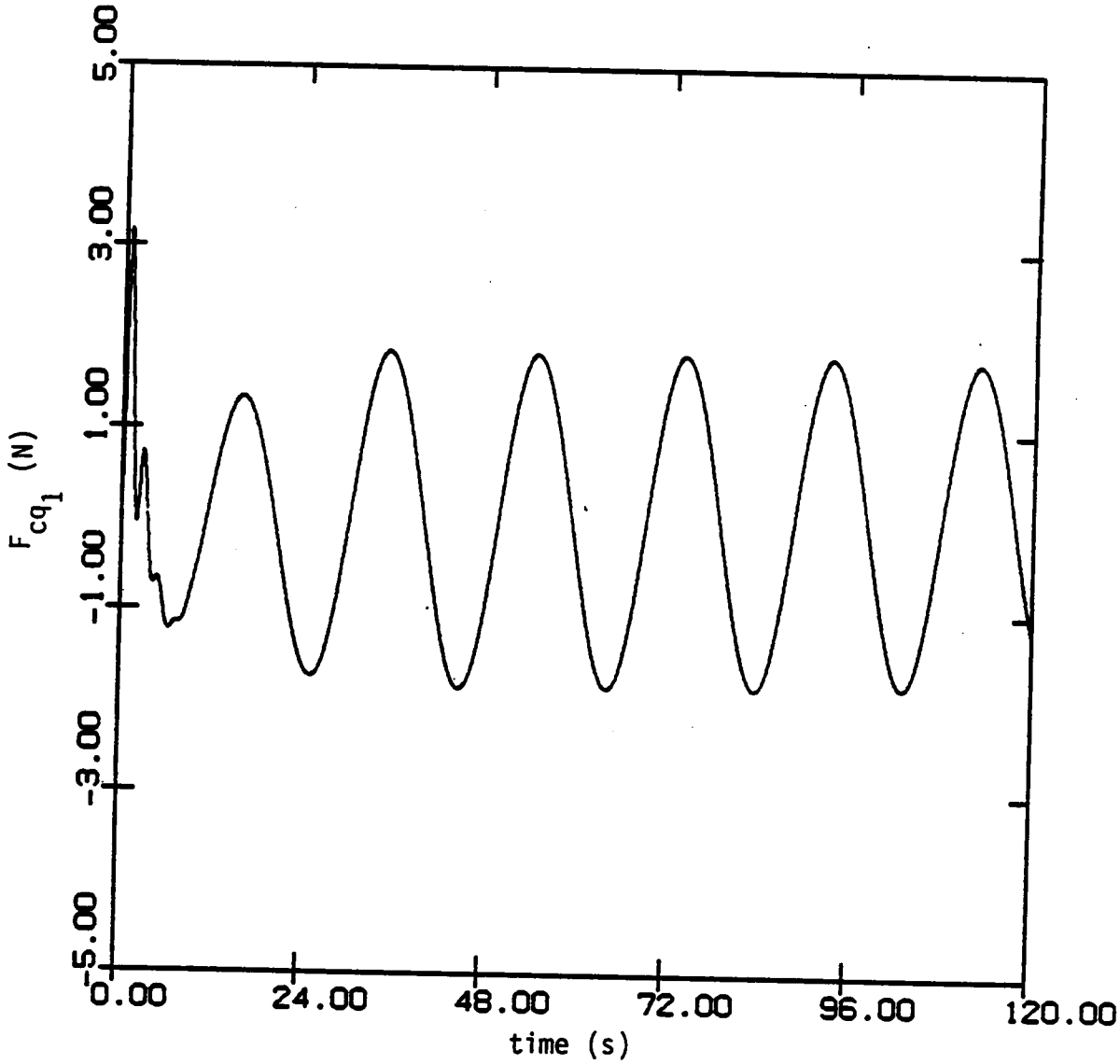

Fig. 5.24 Control Force F_{cq_1} vs Time

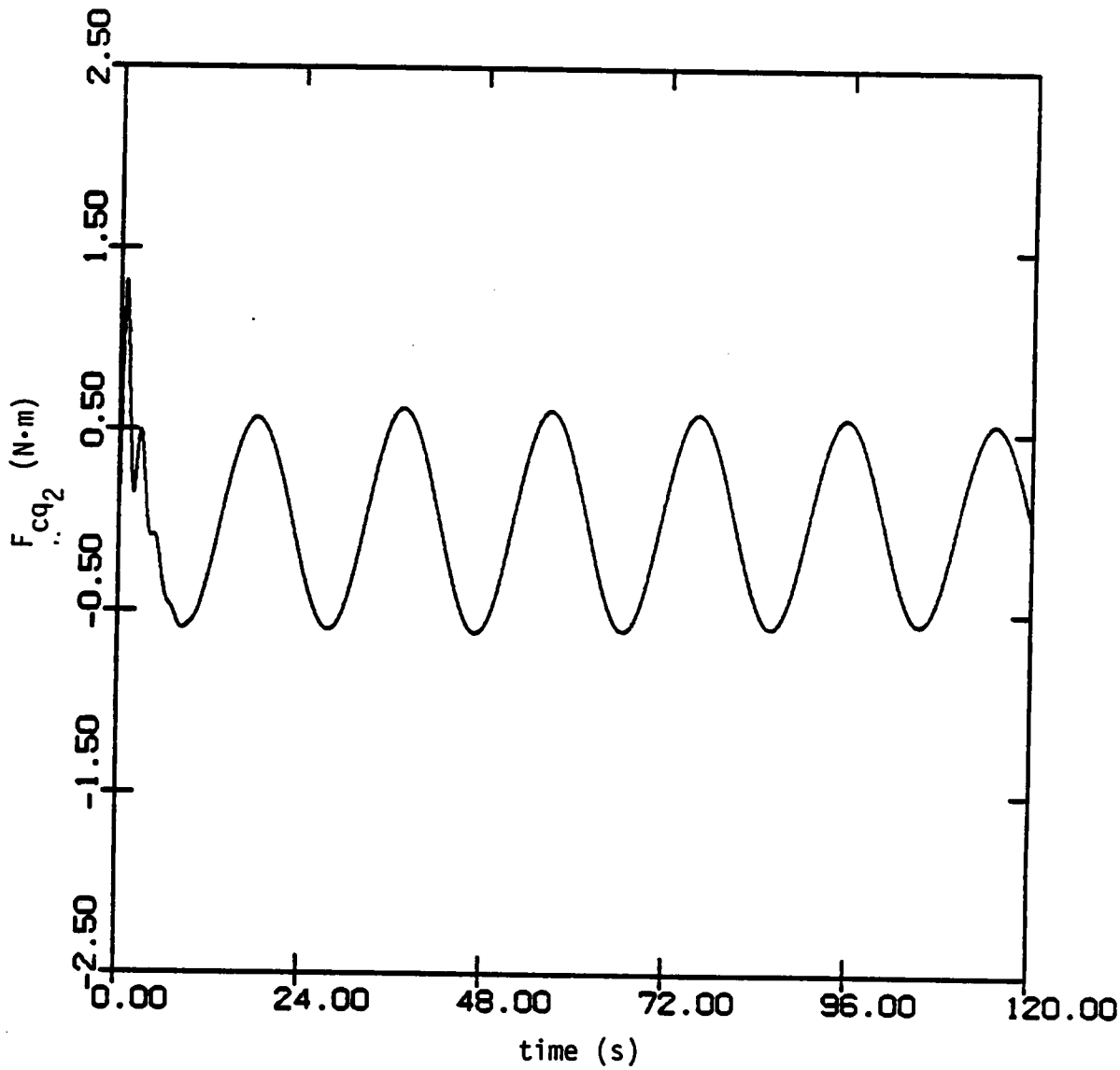

Fig. 5.25 Control Torque F_{cq_2} vs Time

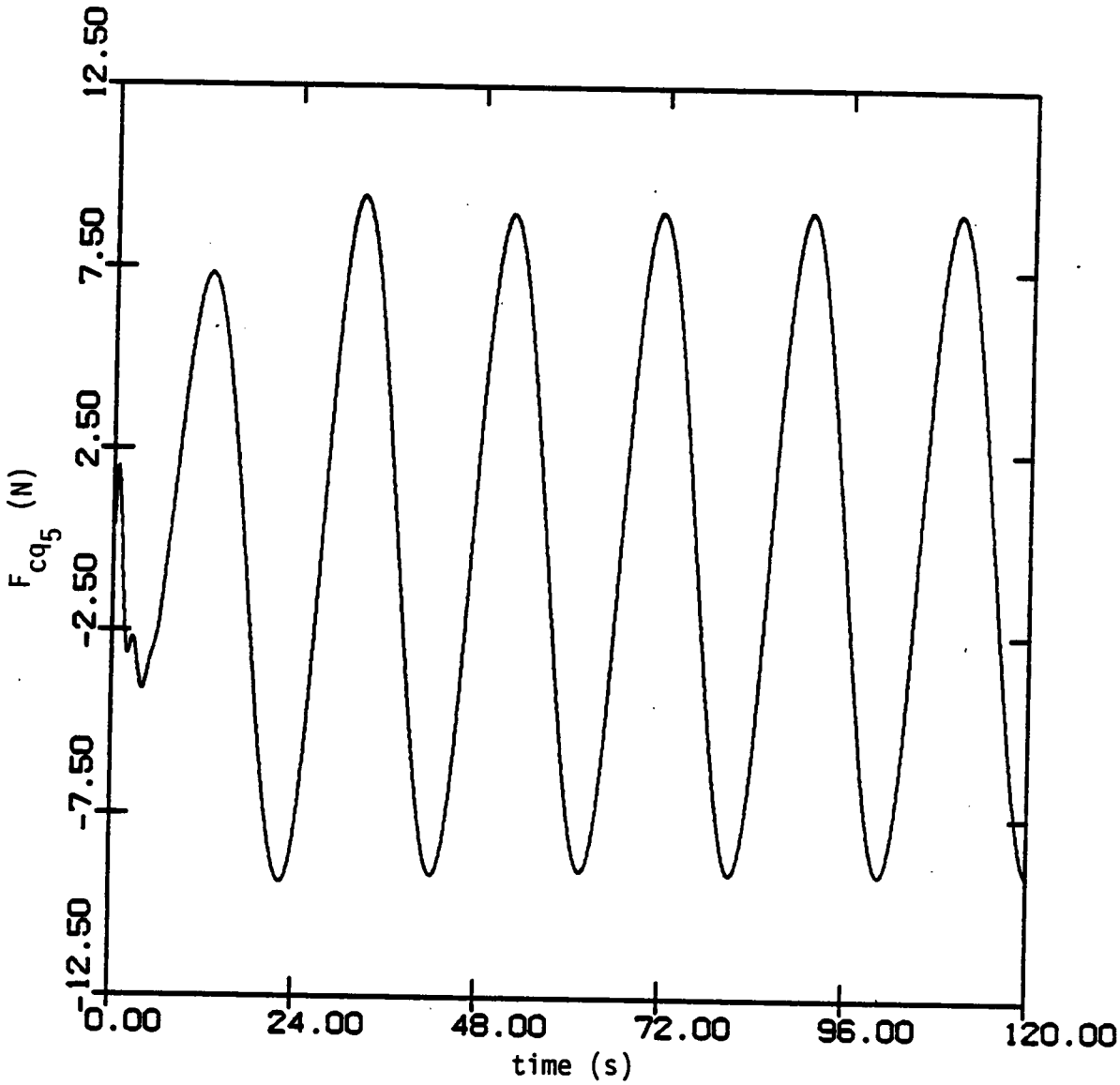

Fig. 5.26 Control Force F_{cq_5} vs Time

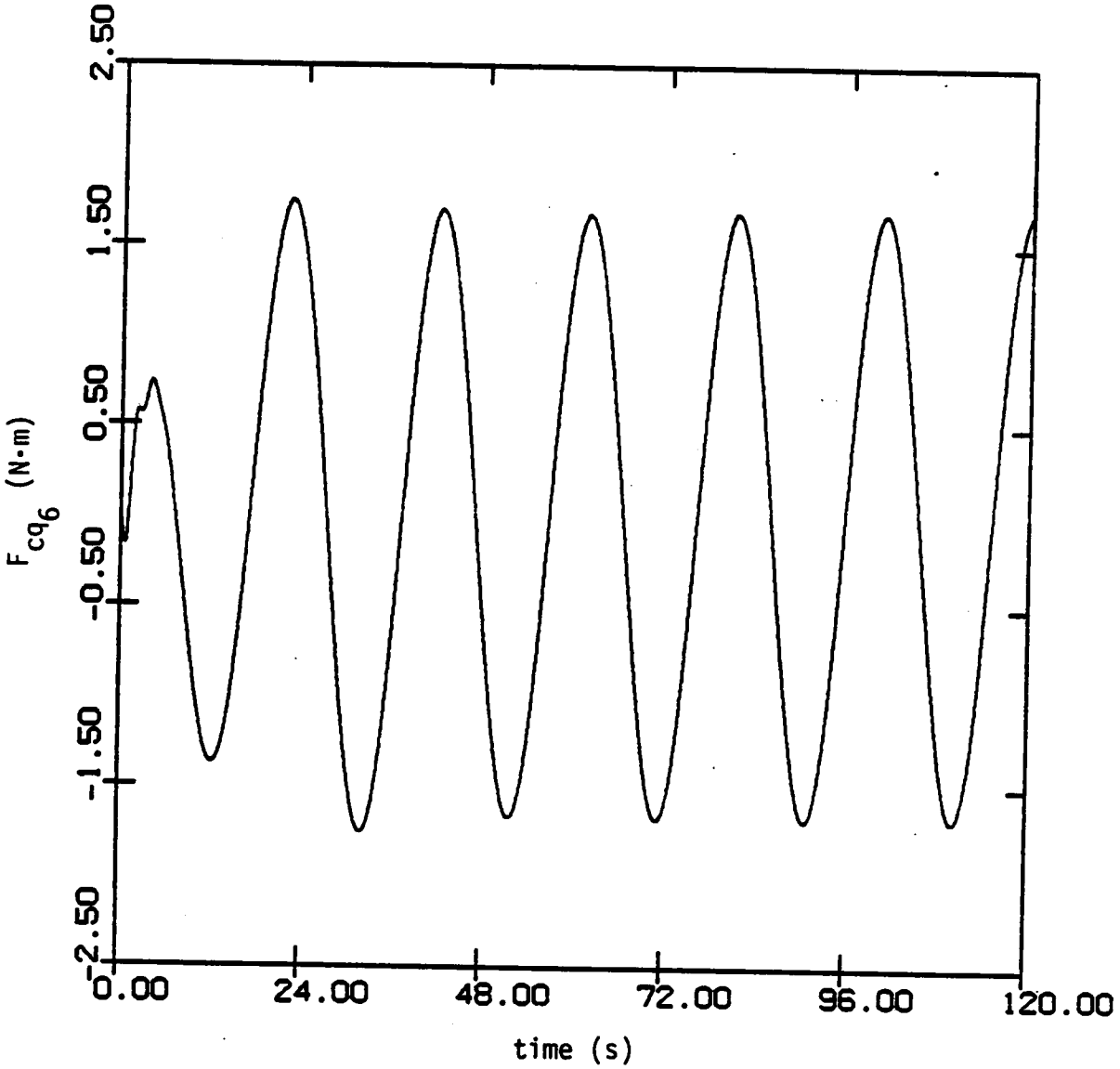

Fig. 5.27 Control Torque F_{cq_6} vs Time

CHAPTER VI

SUMMARY AND CONCLUSIONS

The equations of motion of a semisubmersible structure consisting of a rigid platform and flexible superstructure are derived. The flexible superstructure is discretized by the finite element method and the equations of motion are derived by the Lagrangian approach. For small motions of the structure, the equations are linear. Although in general the excitation forces acting on the structure are due to both wind and waves, only wave-induced vibrations are considered in this dissertation.

It is well known that for a given wave height, the wave energy is distributed according to a Rayleigh distribution. The motion of marine structures cause additional forces which depend on the velocity and acceleration of the structure. The added mass and damping matrices associated with the acceleration and velocity of the structure depend on the frequency of oscillation of the wave. This implies that there is an infinite number of sets of state equations, one for each frequency in the continuous frequency spectrum. Because it is not possible to work with an infinite number of sets of state equations, it is necesary to discretize the frequency spectrum, so that we have as many sets of state equations as increments. A method of discretizing the spectrum, whereby the same amount of energy is allocated to each segment, is shown in Chapter 3. The center frequency (corresponding to one-half of the energy in each segment) is used to calculate the mass and damping matrices of the corresponding segment by assuming that it remains constant within the segment. The center frequency is used to estimate

the amplitude of the wave forces in each segment from precomputed distribution curves. The actual excitation forces for a given segment can be regarded as a sum of the estimated forces and unmodeled forces. Moreover, the unmodeled forces can be regarded as random forces.

The state equations, which are coupled in physical space, are transformed into sets of uncoupled equations in modal space. The eigenvalues of the system consist in general of both real and complex quantities. Real eigenvalues corresponding to rigid-body modes can occur because the semisubmersible is assumed to be unmoored. Control forces are designed in the modal-space. In general the modal equations are coupled through the control forces. When forces are designed by the IMSC approach, the modal equations are both internally (plant) and externally (controller) decoupled. This method, adopted in this dissertation, has distinct computational advantages. For example, the general coupled control method using optimal control involves a large-order Riccati equation. For high-order systems (> 40) this can present severe computational difficulties. In contrast the IMSC method involves only independent sets of first-order or second-order Riccati equations.

The excitation forces, found by discretization of the wave frequency-spectrum, are only a deterministic approximation of the actual wave forces and the responses computed represent estimated values only. To improve the estimates it is necessary to use an observer that takes into account the differences in the measured respones and the estimated responses. The observer eigenvalues are chosen such that the differences in the root-mean-square values of the actual measurements and the estimated measurements are brought down to an acceptable

level. The system eigenvalues and observer eigenvalues are designed separately in accordance with the deterministic separation principle.

Finally, a numerical example is presented. A circular platform with a cantilever beam attached is considered. Control forces and responses are computed for one segment of the spectrum. Also only the velocities at the center of mass of the platform and at the nodal points of the cantilever are measured. Numerical results show that significant reductions (about 50%) in the amplitude of the vibrations are obtained. The differences between the RMS values of the measured velocities and estimated velocities after 120 seconds of simulation are around 10%. In addition to forces due to potential damping, there may be wave drift forces and forces due to currents. Also, the forces due to wind may be significant. It is recommended that these forces be included in future work.

References

1. Bowers, N.A., "Tacoma Narrows Bridge Wrecked by Wind," Engineering News Record, Nov. 14, 1940, pp. 647 and 656.

2. Morgan, M. J., Dynamic Positioning of Offshore Vessels, The Petroleum Publishing Co., Tulsa, Oklahoma, 1978.

3. Balchen, J. G., Jensen, N. A., and Saelid, S. "Dynamic Positioning Using Kalman Filtering and Optimal Control Theory," Automation in Offshore Oil Field Operation, North-Holland Publishing Co., Amsterdam, 1976.

4. Yang, J. "Application of Optimal Control Theory to Civil Engineering Structures," Journal of Engineering Mechanics, ASCE, Dec. 1975, pp 819-838.

5. Meirovitch, L. and Silverberg, L. M., "Control of Structures Subjected to Seismic Excitation," Journal of Engineering Mechanics, Vol. 109, No. 2, April, 1983, pp. 604-618.

6. Meirovitch, L. and Öz, H., "Active Control of Structures by Modal Synthesis," Structural Control, North-Holland Publishing Co., 1980.

7. Meirovitch, L. and Baruh, H., "Optimal Control of Damped Flexible Gyroscopic Systems," Journal of Guidance and Control, Vol. 4, No. 2, 1981, pp. 157-163.

8. Kirk, D. E., Optimal Control Theory, Prentice-Hall Inc., Englewood Cliffs, NJ, 1970.

9. Meirovitch, L., and Ghosh, D., "Control of Flutter in Bridges," International Symposium on Structural Control, Waterloo, Canada, July 1985.

10. Meirovitch, L., Computational Methods in Structural Dynamics, Sijthoff & Noordhoff, The Netherlands, 1980.

11. Pakstys, M., "Dynamic Structural Analysis Techniques for Offshore Platforms," Offshore Technology Conference, Dallas, Texas, 1971.

12. Hooft, J. P., Advanced Dynamics of Marine Structures, John Wiley and Sons, New York, 1982.

13. Potter, J. E., "Matrix Quadratic Solution," SIAM Journal of Applied Mathematics, Vol. 14, p. 496-501, 1966.

14. Brogan, W. L. Modern Control Theory, QPI Publishing, Inc., New York, 1974.

15. Rao, S. S., The Finite Element Method in Engineering, Pergamon Press, Oxford, U.K., 1982.

The vita has been removed from the scanned document